



UNIVERSITY  
IYUNIVESITHI  
UNIVERSITEIT

# **The Design of a PocketQube Satellite Communication System**

Gary Allen  
23905093

November 1, 2023



UNIVERSITEIT•STELLENBOSCH•UNIVERSITY  
jou kennisvennoot • your knowledge partner

## Plagiaatverklaring / *Plagiarism Declaration*

1. Plagiaat is die oorneem en gebruik van die idees, materiaal en ander intellektuele eiendom van ander persone asof dit jou eie werk is.

*Plagiarism is the use of ideas, material and other intellectual property of another's work and to present is as my own.*

2. Ek erken dat die pleeg van plagiaat 'n strafbare oortreding is aangesien dit 'n vorm van diefstal is.

*I agree that plagiarism is a punishable offence because it constitutes theft.*

3. Ek verstaan ook dat direkte vertalings plagiaat is.

*I also understand that direct translations are plagiarism.*

4. Dienooreenkomsdig is alle aanhalings en bydraes vanuit enige bron (ingesluit die internet) volledig verwys (erken). Ek erken dat die woordelikse aanhaal van teks sonder aanhalingstekens (selfs al word die bron volledig erken) plagiaat is.

*Accordingly all quotations and contributions from any source whatsoever (including the internet) have been cited fully. I understand that the reproduction of text without quotation marks (even when the source is cited) is plagiarism*

5. Ek verklaar dat die werk in hierdie skryfstuk vervat, behalwe waar anders aangedui, my eie oorspronklike werk is en dat ek dit nie vantevore in die geheel of gedeeltelik ingehandig het vir bepunting in hierdie module/werkstuk of 'n ander module/werkstuk nie.

*I declare that the work contained in this assignment, except where otherwise stated, is my original work and that I have not previously (in its entirety or in part) submitted it for grading in this module/assignment or another module/assignment.*

Studentenommer / <i>Student number</i>	Handtekening / <i>Signature</i>
Voorletters en van / <i>Initials and surname</i>	Datum / <i>Date</i>

# Contents

<b>Declaration</b>	i
<b>List of Figures</b>	vi
<b>List of Tables</b>	viii
<b>Abstract</b>	x
<b>1. Introduction</b>	1
1.1. Overview . . . . .	1
1.2. Problem Statement . . . . .	2
1.3. Requirements . . . . .	2
1.4. Specifications . . . . .	3
<b>2. Background</b>	5
2.1. PocketQube . . . . .	5
2.2. Satellite Tracking . . . . .	5
2.2.1. Open-Loop . . . . .	6
2.2.2. GPS (Direct) . . . . .	6
2.2.3. GPS (Relay) . . . . .	6
2.2.4. Signal Strength . . . . .	7
2.3. Antennas . . . . .	7
2.3.1. Types . . . . .	7
2.3.2. Feedlines . . . . .	10
2.3.3. Summary . . . . .	11
2.4. Telecommunication . . . . .	11
2.4.1. Modulation Techniques . . . . .	11
2.4.2. Link Budget . . . . .	12
2.4.3. Protocols . . . . .	12
<b>3. System Design</b>	13
3.1. High-Level System . . . . .	13
3.1.1. Methodology . . . . .	13

3.1.2. Tracking . . . . .	13
3.1.3. Custom Link . . . . .	14
3.2. Ground Station . . . . .	14
3.2.1. Power . . . . .	14
3.2.2. Communication . . . . .	14
3.2.3. Steering and Positioning . . . . .	15
3.2.4. Monitoring . . . . .	16
3.3. PocketQube Unit . . . . .	16
<b>4. Detailed Design</b>	<b>17</b>
4.1. Component Selection . . . . .	17
4.1.1. GPS . . . . .	17
4.1.2. IMU . . . . .	17
4.1.3. RF Module . . . . .	18
4.1.4. Stepper Motor Driver . . . . .	19
4.1.5. Power . . . . .	19
4.1.6. Microcontroller . . . . .	20
4.1.7. RS-485 Driver . . . . .	20
4.2. Ground Station PCB . . . . .	20
4.2.1. Circuit Design . . . . .	20
4.2.2. PCB Design . . . . .	21
4.3. PocketQube Unit PCB . . . . .	22
4.3.1. Circuit Design . . . . .	22
4.3.2. PCB Design . . . . .	23
4.4. Link Budget . . . . .	23
4.5. Ground Station Antenna . . . . .	25
4.5.1. Mechanical Considerations . . . . .	25
4.5.2. Theoretical Design . . . . .	26
4.5.3. Simulation Design . . . . .	27
4.5.4. Matching . . . . .	30
4.6. PocketQube Unit Antenna . . . . .	31
4.6.1. Mechanical Considerations . . . . .	31
4.6.2. Simulation Design and Matching . . . . .	31
4.7. Software . . . . .	32
4.7.1. Classes . . . . .	32
4.7.2. Tracking . . . . .	33
<b>5. Implementation</b>	<b>34</b>
5.1. Ground Station PCB . . . . .	34
5.2. Ground Station Antenna . . . . .	34
5.3. PocketQube Unit PCB . . . . .	35

5.4. PocketQube Unit Antenna . . . . .	36
5.5. Software . . . . .	36
5.5.1. Mount Control . . . . .	36
5.5.2. Pointing . . . . .	37
5.5.3. Radio and GPS . . . . .	37
5.5.4. GUI . . . . .	37
<b>6. Testing</b>	<b>38</b>
6.1. Ground Station PCB . . . . .	38
6.1.1. Power . . . . .	38
6.1.2. Motor Drive . . . . .	38
6.2. PocketQube Unit PCB . . . . .	39
6.3. Ground Station Antenna . . . . .	39
6.4. PocketQube Unit Antenna . . . . .	40
6.5. RF Module . . . . .	40
6.5.1. Setup . . . . .	40
6.5.2. Transmit Power Consumption . . . . .	41
6.5.3. Data Rate . . . . .	41
6.6. Serial Protocol . . . . .	42
6.7. Range . . . . .	42
6.8. Tracking and Pointing . . . . .	44
6.8.1. Open-Loop . . . . .	44
6.8.2. Closed-Loop . . . . .	45
6.9. Radiosonde . . . . .	46
6.10. Full System . . . . .	46
<b>7. Conclusion</b>	<b>47</b>
7.1. Summary . . . . .	47
7.2. Future Work . . . . .	47
<b>Bibliography</b>	<b>49</b>
<b>A. Project Planning</b>	<b>53</b>
<b>B. References</b>	<b>54</b>
B.1. PQSU . . . . .	54
B.2. SUNCQ . . . . .	55
B.3. Antenna Gain . . . . .	57
<b>C. Design</b>	<b>58</b>
C.1. Ground Station Schematic . . . . .	58
C.2. PocketQube Unit Schematic . . . . .	59

C.3. Ground Station PCB . . . . .	60
C.4. PCB Errata . . . . .	60
C.5. Software . . . . .	60
<b>D. Hardware</b>	<b>62</b>
D.1. Existing Mount PCB . . . . .	62
D.2. PocketQube . . . . .	63
D.3. Mount Rotation . . . . .	64
<b>E. Software</b>	<b>65</b>
E.1. GUI . . . . .	65
<b>F. Tests</b>	<b>66</b>
F.1. Range Tests . . . . .	66

# List of Figures

1.1. A High-Altitude Balloon Carrying a Nano-Satellite Payload [1] . . . . .	1
1.2. Predicted Balloon Path and Distances . . . . .	2
2.1. A CAD Model of a PQSU Enclosure [2] . . . . .	5
2.2. GPS Relay Tracking [3] . . . . .	7
2.3. Dipole Antenna Geometry . . . . .	8
2.4. Dipole Antenna Radiation Pattern . . . . .	8
2.5. A Monopole Whip Antenna in a Plastic Housing . . . . .	8
2.6. A 21-turn Copper Helical Antenna . . . . .	8
2.7. Yagi-Uda Antenna Geometry [4] . . . . .	9
2.8. Two Inverted-F Microstrip Antenna Geometries [5] . . . . .	9
3.1. High-Level System Diagram . . . . .	13
3.2. Groud Station System Diagram . . . . .	15
3.3. Azimuthal and Elevation Visualization [6] . . . . .	15
3.4. The Existing Antenna Mount . . . . .	15
3.5. PocketQube Unit System Diagram . . . . .	16
4.1. PocketQube Unit PCB Design (Front) . . . . .	23
4.2. PocketQube Unit PCB Design (Back) . . . . .	23
4.3. Initial Simulated Helical Antenna Radiation Pattern ( $f = 550 \text{ MHz}$ ) . . . . .	27
4.4. Simulated Helical Antenna Pattern at $f = 405 \text{ MHz}$ ( $f_c = 550 \text{ MHz}$ , $G_\lambda = 0.5$ ) . . . . .	28
4.5. Simulated Helical Antenna Pattern at $f = 405 \text{ MHz}$ ( $f_c = 550 \text{ MHz}$ , $G_\lambda = 0.7$ ) . . . . .	28
4.6. Simulated Helical Antenna Input Impedance ( $f_c = 550 \text{ MHz}$ , $G_\lambda = 0.7$ ) . . . . .	28
4.7. Simulated Helical Antenna Input Impedance ( $f_c = 510 \text{ MHz}$ , $G_\lambda = 0.6$ ) . . . . .	29
4.8. Simulated Helical Antenna Pattern without Cup ( $G_\lambda = 0.6$ , $f = 405 \text{ MHz}$ ) . . . . .	29
4.9. Simulated Helical Antenna Pattern with Cup ( $G_\lambda = 0.6$ , $f = 405 \text{ MHz}$ ) . . . . .	29
4.10. Helical Antenna with Matching Strip Simulation Model . . . . .	30
4.11. Simulated Helical Antenna Return Loss vs Frequency . . . . .	30
4.12. General Dipole Simulation Model . . . . .	32
4.13. Simulated $0.45\lambda$ Dipole Radiation Pattern . . . . .	32
4.14. Simulated $0.45\lambda$ Dipole Return Loss vs Frequency . . . . .	32

4.15. Tracking Algorithm Flow Diagram . . . . .	33
5.1. Ground Station PCB Implementation . . . . .	34
5.2. Ground Station Initial Antenna Implementation . . . . .	34
5.3. Ground Station Mounted on Tripod . . . . .	35
5.4. PQ Unit (front) [right] and programmer [left] . . . . .	36
5.5. PQ Unit (back) . . . . .	36
6.1. Measured Helical Antenna Return Loss vs Frequency . . . . .	40
6.2. Measured Dipole Antenna Return Loss vs Frequency . . . . .	41
6.3. TX Output Power vs Current Consumption . . . . .	41
6.4. Measured RSSI vs Distance . . . . .	43
6.5. Measured SNR vs Distance . . . . .	43
6.6. Pointing Test Setup . . . . .	44
6.7. GPS Tracking Locations and RSSI Values . . . . .	45
6.8. Received Radiosonde Signal FFT . . . . .	46
B.1. Antenna Gain vs Beamwidth [7] . . . . .	57
C.1. Ground Station PCB Design . . . . .	60
D.1. Existing Antenna Mount PCB . . . . .	62
D.2. PocketQube Breadboard for Testing . . . . .	63
D.3. PocketQube Dipole Antenna . . . . .	63
D.4. Mount Azimuthal Compensation 1 (Elevation Fixed) . . . . .	64
D.5. Mount Azimuthal Compensation 2 (Elevation Fixed) . . . . .	64
D.6. Mount Azimuthal Compensation 3 (Elevation Fixed) . . . . .	64
D.7. Mount Azimuthal Compensation 4 (Elevation Fixed) . . . . .	64
D.8. Mount Azimuthal Compensation 5 (Azimuth Fixed) . . . . .	64
D.9. Mount Azimuthal Compensation 6 (Azimuth Fixed) . . . . .	64
E.1. GUI Snapshot . . . . .	65
F.1. Range Test Locations . . . . .	66

# List of Tables

2.1.	Qualitative Comparison of Antenna Characteristics [8]	11
4.1.	Comparison of two LoRa modules	19
4.2.	Ground Station Component Power Consumption	21
4.3.	PocketQube Unit Component Power Consumption	22
4.4.	Notable SX1278 Configurations	24
4.5.	Link Budget - Satellite	24
4.6.	Link Budget - Channel	24
4.7.	Link Budget - Ground Station	24
4.8.	Mount Gear and Motor Specifications	25
4.9.	Helical Antenna Final Parameters	31
6.1.	Ground Station Voltage Measurements	38
6.2.	Motor Drive Operating Tests @ 12 V supply	39
6.3.	LoRa Bit Rate vs Spreading Factor	42
6.4.	Range Test Locations	42
C.1.	GPS Class	60
C.2.	Radio Class	60
C.3.	Link Class	61
C.4.	StepperMotor Class	61
C.5.	Mount Class	61
C.6.	GroundStation Class	61

# Nomenclature

## Acronyms and abbreviations

ACK	Acknowledge
ASK	Amplitude Shift Keying
CAD	Computer-Aided Design
CCSDS	Consultative Committee for Space Data Systems
CRC	Cyclic Redundancy Check
CSP	CubeSat Space Protocol
EIRP	Equivalent isotropic radiated power
EPS	Energy Power System
FSK	Frequency Shift Keying
GFSK	Gaussian Frequency Shift Keying
GNNS	Global Navigation Satellite System
GPS	Global Positioning System
GS	Ground Station
GUI	Graphical User Application
IC	Integrated Circuit
IMU	Inertial Measurement Unit
LEO	Low Earth Orbit
LOS	Line-of-Sight
PCB	Printed Circuit Board
PQ	PocketQube
PQSU	PocketQube Stellenbosch University
PEC	Perfect Electrical Conductor
PSK	Phase Shift Keying
QAM	Quadrature Amplitude Modulation
RF	Radio Frequency
RX	Receive
SF	Spreading Factor
SU	Stellenbosch University
TX	Transmit

# Abstract

## English

This report documents the design and implementation of a wireless communication system for a miniaturised satellite called a *PocketQube*. The PocketQube standard is a set of specifications which aim to make it easier for people to design small satellite modules that can easily integrate with each other. The standard is relatively new, however, and few designs have been published for a full PocketQube communication system that includes a ground station.

The design in this project includes both a tracking ground station, as well as a PocketQube module. The LoRa-based ground station was designed to mechanically track the satellite system using a pre-defined GPS path, as well as using satellite-received GPS data. The system was then implemented, and the communication link was tested up to 100 km line-of-sight and found to be reliable at a baud rate of 9600 bps. This report documents the design choices made and constraints faced, analyses the measured results of the system, and suggests improvements for future projects.

# 1. Introduction

## 1.1 Overview

This project aims to design and implement a wireless communication system for a miniaturised satellite called a *PocketQube* (PQ). The PocketQube standard was created to define physical and electronic requirements for so-called “nano-satellites”, with the goal of easy integration of various sub-modules into one physical enclosure.

Nano-satellites can either be placed into orbit, or attached to a *high-altitude balloon*. One common use-case of these balloons is to collect sensory information from the atmosphere, such as temperature and humidity readings. The goal of this project is to design a system that can be used in a balloon launch from the Saldanha Air Field, which may ultimately be done by the Stellenbosch Engineering department.



**Figure 1.1:** A High-Altitude Balloon Carrying a Nano-Satellite Payload [1]

A satellite communication system includes both a ground station (GS), as well as a module on the satellite itself. The aim of this project is to establish a minimal prototype for both of these systems, so that future projects can refine the developed sub-systems. In this report, general system requirements are first listed, and a problem statement is drawn up. Then, a literature review is conducted to gather background information in the fields of interest. This includes an overview of the PocketQube standard, antenna theory, satellite tracking, and telecommunication theory. A systems level design is then done, which is followed by a more detailed design. Finally, the system is implemented and tested, the results are discussed, and potential improvements and work for future projects are listed.

## 1.2 Problem Statement

The initial problem statement was simply to design a communication system for a PocketQube, with focus on the ground station. As this is relatively broad, further investigation of existing balloon-satellite systems, as well as the launch for this specific PocketQube, was done. An additional requirement that the GS should be capable of receiving information from an existing *Radiosonde* (an atmospheric telemetry device) was also given, as a backup link. The existing radiosonde (an iMet-54) is therefore used as a reference, both for the new system's requirements, and as a consideration for system integration.

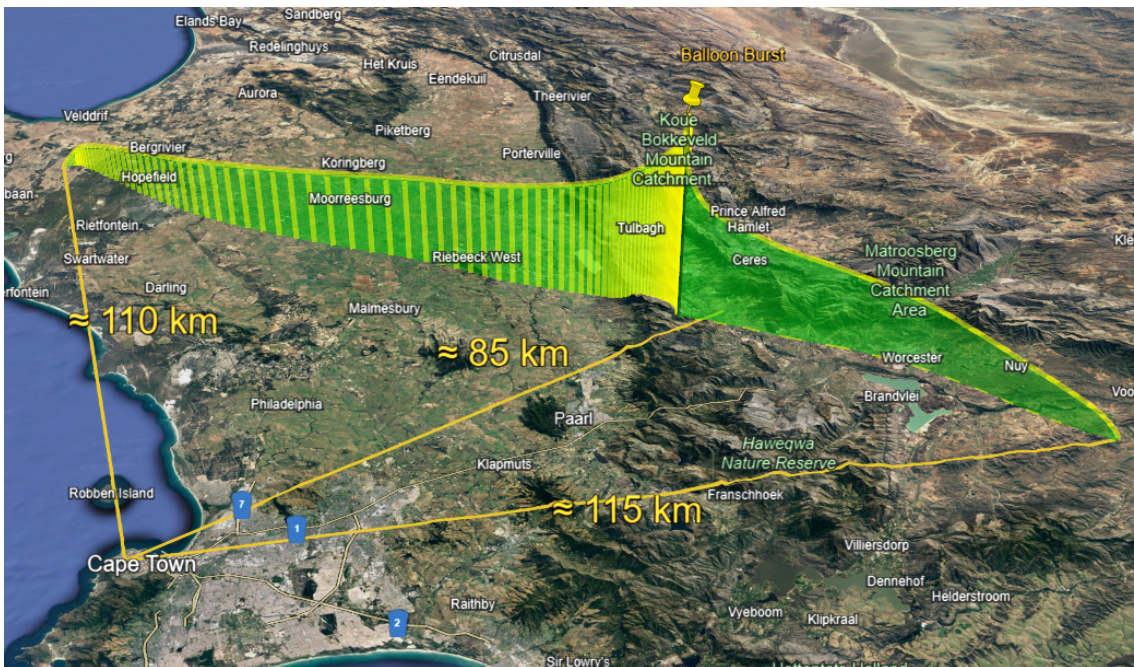


**Figure 1.2:** Predicted Balloon Path and Distances

High-altitude balloons can drift to a height as much as 30 km above sea level, and can drift as far as 200 km from launch [9]. As mentioned, this project's launch is planned to be near Saldanha Airfield. Using the *HabHub* path predictor [10] on a day where the balloon travels far in-land, a launch from the airfield results in the path as in Figure 1.2. From Cape Town, this is a maximum straight line distance of around 115 km.

A ground station should maintain a reliable wireless link with a satellite to enable continuous communication and real-time telemetry. Since most radiosondes are simply uni-directional "downlink" devices, this should be a priority requirement, however the GS should also be capable of bi-directional communication, in order to issue commands to the satellite.

## 1.3 Requirements

From the information listed in the problem statement, and after supervisor consultation, slightly more specific user requirements are gathered and listed:

1. The GS should be capable of receiving continuous data wirelessly from the PQ and the Radiosonde. The PQ should be capable of responding to commands from the GS.
2. The communication link should be maintained throughout the predicted path covered in Figure 1.2
3. The PQ unit should remain operational for at least the launch time of the predicted path, which is 2 hours 25 minutes. To cater for longer flights, a goal of 3 hours is set.
4. The PQ unit should conform to the *SU-modified* PQ9 standard (listed in Appendix B.1), and integrate with other prototype units. This standard is here-on referred to as *PQSU*.
5. The GS electronics should integrate into an existing antenna mount, which has been provided by the Department.

The system will undergo a *flight-readiness review* to determine if it has met the requirements before launch. Although the GS could be placed closer to the launch location if the range requirement is not met (while affecting the communication time) this should only be used as a last resort. Further, as the project progresses, if supporting greater distances ( $> 200$  km) will not significantly increase the time, complexity, or cost of the system, it could be catered for as an expansion to the core requirements. It should be noted, however, that the nature of this project (a system prototype) means that such optimisations should not be made a priority.

## 1.4 Specifications

In order to define a more detailed list of specifications, further calculations should be done. Balloon satellites rise at a vertical speed of around 20 km/h, and safely fall at around 35 km/h after bursting if a parachute is used [9]. The predicted flight path in Figure 1.2 shows a traveled horizontal distance of about 60 km in 40 minutes after the balloon bursts, resulting in a horizontal speed of 90 km/h. A speed of around 100 km/h will be designed for to cater for slightly faster fall speeds.

At a maximum height of 30 km, a calculator reveals that the horizon is around 600 km [11]. The GS antenna could therefore be placed at sea level if communication is only required near maximum altitude. If the requirement is set that the balloon should instead be tracked within one minute after launch (300 metres), then a radar horizon calculator reveals that the GS should be placed at an altitude no lower than 200 metres [12], assuming no refraction.

Again referring to the predicted path, a maximum slant range of just over 115 km is obtained, noting that the balloon moves closer as it increases in altitude. For simplification, if the maximum speed (28 m/s) is assumed to occur perpendicular to the ground station at this maximum range, a turn-rate requirement of  $t = \frac{v}{r} = \frac{28}{115000} \approx 0.015^\circ/s$  is obtained. Due to this loose requirement, an additional constraint is added to require the ground station to track at  $\approx 2.5^\circ/s$ , to cater for low-earth orbit satellites moving at 8 km/s at 200 km altitude.

The PQSU standard includes 3.3V and 5V bus voltages. Since this is a prototype launch, there is risk of other units (e.g. the EPS) malfunctioning. A power connection is also needed for development. A simple battery system which matches the PQSU voltage should therefore be included, to be used both for testing, and potentially for deployment.

Both systems will require PCBs which are constrained in size. PQSU defines the dimensions of a PocketQube PCB i.e. 42 mm x 42 mm outer dimensions, whereas the ground station PCB is constrained to fit onto the provided mount with similar sizing as the previous PCB that was used with it, as shown in Appendix D.1. Lastly, the system should drive the stepper motors which are already provided with the antenna mount, and may make use of the existing zero-sensor. The following system-level specifications are therefore drawn up:

1. The system should be capable of a slant range of 120 km.
2. The GS should be capable of tracking at a turning rate of  $2.5^\circ/s$ , and the feasibility of various tracking methods (e.g. open vs closed loop) should be explored.
3. The system should be designed to operate at a minimum baud rate of 4800 (which the iMet-54 uses [13]) and a target baud rate of 9600 (which is a typical satellite telemetry downlink speed as in [14]).
4. The system should allow for iMet-54 radiosonde data to be retrieved. This data is GFSK modulated at a pre-selected frequency of between 402 to 405 MHz [13].
5. A single antenna should be used for both the custom and radiosonde link on the GS, to simplify the design. This antenna should therefore have a bandwidth in the range from 405 MHz up to the amateur radio band (433 MHz).
6. A 100 mW equivalent transmit power restriction should be adhered to.
7. The PQ unit should follow the PQSU and PQ9 standards, which stipulates: a 42 mm square outer PCB dimension; a 4 mm and 2 mm component height above and below respectively; and a 20-pin header interface, catering for RS-485 and I2C communication, and providing 3.3 V and 5 V power lines.
8. The PQ unit should include a battery capable of lasting a minimum of 3 hours at nominal current draw.
9. The GS PCB should integrate onto the existing antenna mount, which has a diameter of 198 mm, with equispaced mounting holes of 3 mm diameter.
10. The GS should be mechanically steered using 4218S-15 bipolar stepper motors, which have a maximum current of 0.50 A per phase, and are driven at 24 V.
11. The GS should provide a USB-C connection to allow a PC to monitor the telemetry data. This should be capable of receiving all data from the link in real-time.

## 2. Background

### 2.1 PocketQube

The PocketQube standard is a fairly new set of protocols and specifications defining a modularized nano-satellite system. The term *modularized* in this context refers to the ability for different “modules” or PocketQube units, each with their own set functionality, to be connected to a common *backplane* and integrated seamlessly. *Integration* here refers to both the mechanical spacing of each module, as well as the electronic communication between the modules.

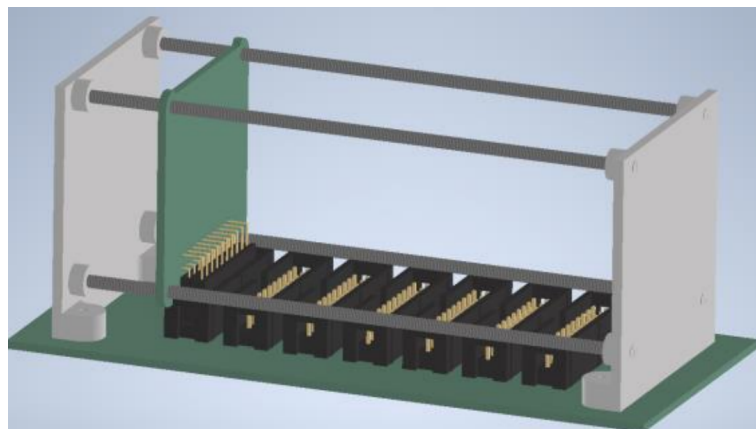


**Figure 2.1:** A CAD Model of a PQSU Enclosure [2]

As an example, a PocketQube enclosure could contain three units: a communication module, a sensor pack, and a battery system. These modules can then be connected onto a PCB backplane via headers, placed inside a single enclosure, such as that in Figure 2.1, and either launched or released appropriately.

### 2.2 Satellite Tracking

There are various methods used to track satellites in order to maintain communication. Ultimately, all of these methods provide a single input to the ground station system: the direction in which to “steer” its antenna. Each method is compared and expanded on below.

### 2.2.1 Open-Loop

Arguably the simplest tracking method is using what may be referred to as “open-loop” control. Here, only information about the predicted flight path of the balloon/satellite is used, such as expected GPS co-ordinates at different points in time.

Given co-ordinates of both the ground station and the satellite (provided in the *WGS84* system), *Mercator projection* can be used to obtain a cartesian pointing vector [15]. The ground station can then simply be pointed in that direction at each instant in time. The flight path can either be a pre-calculated path (as demonstrated in Figure 1.2), or can be continuously re-estimated based on real-time weather data. *Habhub* is an online high-altitude path predictor [16] which is freely available.

An advantage of this method is its extreme simplicity to implement. It has several disadvantages, however, including being vulnerable to prediction inaccuracies, as well as the difficulty experienced in re-acquiring the communication link once it is lost. Further, a GPS receiver is generally still required on the ground station, unless it is positioned with a pre-determined location and orientation.

### 2.2.2 GPS (Direct)

If an initial communication link can be established between the satellite and ground station, *direct* GPS transmission can be added for positional feedback. This is a simple method of “closing” the tracking loop, since the path data can be updated dynamically. Generally, both the PQ and GS GPS co-ordinates are required.

### 2.2.3 GPS (Relay)

If a link cannot be initially established, a ”relay” method of GPS tracking can be used. This method functions in a three-step process, explained below and depicted in Figure 2.2:

1. The precise position of the payload and the ground station is determined using data received from GPS satellites.
2. The position is *relayed* to an external network (satellite or ground-based) using a radio transmitter.
3. The ground station receives the location from the external network (e.g. via the internet).

The major disadvantage of this method is the additional cost required. Since an antenna capable of communicating with one of the external networks is required, two antennas are needed if direct communication with a ground station is desired (however this is usually no longer necessary as the relay network can be used). Further, the cost of subscribing to an external network is generally high.

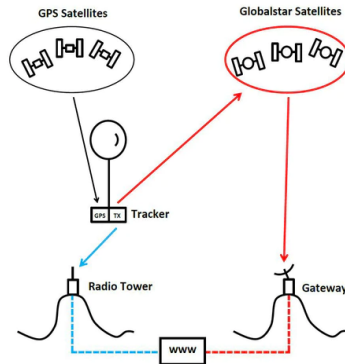


**Figure 2.2:** GPS Relay Tracking [3]

This type of tracking works well if the satellite is physically close to the external network satellites, or if the ground station does not need to communicate in real-time, but merely needs access to the location of the satellite e.g. in a home-made balloon satellite launch.

## 2.2.4 Signal Strength

Radio tracking can be done when the satellite itself transmits omni-directionally. The received signal strength can be used as feedback to determine the direction to point. To initially find the satellite, the entire sky can be scanned using a "brute force" procedure, or an initial guess can be provided. Then, periodic *radius scanning* can be used to track the signal within a certain portion of the sky, or more advanced techniques such as *conical scanning* can be used, to calculate a new direction to point given a set of conically signal strength measurements.

This method provides great flexibility, since no satellite path information is required, however it is generally not necessary when a reasonable initial guess is available, and an antenna with a reasonably large beamwidth is used.

## 2.3 Antennas

This section covers a very brief review of different types of antennas in literature, as well as how to practical feed these antennas with a transmission line, and a summary of their varying performances.

### 2.3.1 Types

There are various antenna types to consider for a satellite communication system. A highly customized design is out of the scope of this project, and therefore only designs with tunable parameters, or existing designs in literature, will be considered. Ultimately, each antenna's *radiation pattern*, *gain* (dBi i.e. decibels relative to an *isotropic* source); fractional *bandwidth*; main lobe *beamwidth*; dimensions; and polarization will be compared. Here, *polarization* refers to the orientation of the EM wave i.e. horizontal, vertical or circular.

### Half-Wavelength Dipole

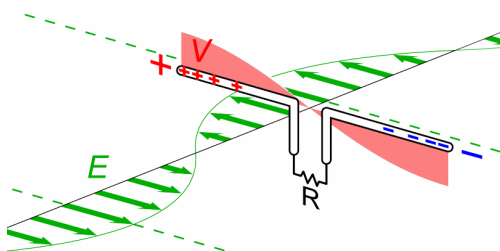


**Figure 2.3:** Dipole Antenna Geometry

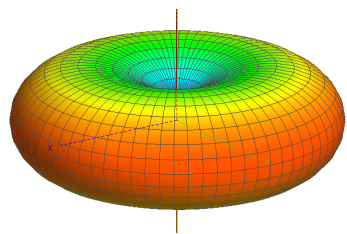


**Figure 2.4:** Dipole Antenna Radiation Pattern

The half-wavelength ( $0.5\lambda$ ) dipole antenna is arguably the simplest and most common type of antenna. It consists of two conductive elements operating in opposite phase, as depicted in Figure 2.3. It is described to have a donut-shaped radiation pattern as in Figure 2.4, with *omni-directional* radiation in the plane perpendicular to the conductor, and a *null* tangential to the conductor. It has a maximum gain of 2.15 dBi, and is linearly polarized. [8]

### Quarter-Wave Monopole

The working principle of a monopole antenna makes use of the electromagnetic theory of *imaging*. If an infinite ground plane or Perfect Electrical Conductor (PEC) is placed below one half of a  $0.5\lambda$  dipole antenna, since the PEC holds the constraint that the tangential electric field is zero across its boundary, an equal but opposite electromagnetic wave is “induced” due to the incident wave. This wave “appears” to have come from an equal but oppositely polarized “image” source, hence removing the need for the second half of the dipole to be present.

These antennas are extremely useful when size is a constraint, however have the disadvantage of requiring a ground plane. A *whip* antenna is a form of monopole antenna designed to be flexible so that it does not break as easily, and often without a ground plane with reduced performance. It is often placed inside a plastic enclosure, as in Figure 2.5. [8]



**Figure 2.5:** A Monopole Whip Antenna in a Plastic Housing



**Figure 2.6:** A 21-turn Copper Helical Antenna

## Helical

Helical antennas are coiled windings of wire, where the circumference of the coil has some relationship with the desired frequency. Commonly, a circumference of  $C = 1.0\lambda$  is used for *uni-directional* or *axial mode* variants. In this case, a ground plane is required. The ground plane can also be *capped* (i.e. extended as an open cylinder) for additional directivity [17]. *Omni-directional* or *normal mode* variants are possible without a ground plane, when  $C \ll \lambda$ . Figure 2.6 depicts a 21-turn example of such an antenna.

Helical antennas have several design parameters that influence the antenna's characteristics, such as number of turns ( $n$ ), wire width ( $wd$ ), and spacing between turns ( $S$ ). A spacing of  $0.20\lambda < S < 0.25\lambda$  is recommended, however smaller spacings of  $0.10\lambda < S < 0.20$  are commonly used [18]. These antennas are also capable of either linear or circularly polarized signals. Lastly, since they can be designed with an arbitrarily small or large number of turns, and they have a large operating bandwidth, they can be made smaller than other alternatives.

## Patch

A *patch* or *PCB* antenna is simply a rectangular PCB trace sized correctly to allow for radiation. Typically, a simple square or rectangular shape can be used. They allow for small profiles at the cost of efficiency [8], and either have circular or linear polarization.

## Array

In general, multiple antennas can be combined in an *array* configuration. This allows complete manipulation of the design (such as the desired gain), by virtue of *constructive* and *destructive* interference of the electromagnetic waves. Common variations of this concept reside in *Yagi-Uda* and *Patch Array* antennas. [8]

## Yagi-Uda

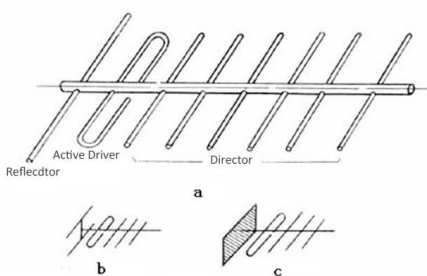


**Figure 2.7:** Yagi-Uda Antenna Geometry [4]

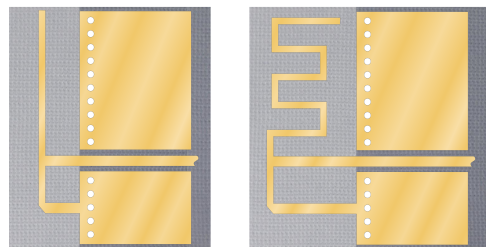


**Figure 2.8:** Two Inverted-F Microstrip Antenna Geometries [5]

Although not strictly an antenna array, *Yagi-Uda* antennas are one of the most popular directive antennas that make use of interference. A given number of passive conductors are

stacked in a specific configuration as shown in Figure 2.7, ultimately steering the EM waves using the concept of interference. Only one of the conductors in the array is fed with the signal. They generally can be made to have very large gain, and are linearly polarized. A *cross-yagi* is a variation on this design which allows for circular polarization.

### **Microstrip**

*Microstrip* antennas generally refer to any planar, PCB antenna. They can be considered a generalization of a patch antenna. Many variations exist due to their flexible nature. A few examples include a: a *patch array*; an *inverted-F* design, which has a small form factor and a nearly 3D omni-directional radiation pattern; a *ring antenna* [19], which is uni-directional, and has an even smaller form factor than the inverted-F antenna; and a *helical patch* antenna, which is simply a "zig-zag" helix shape flattened onto a PCB.

### **2.3.2 Feedlines**

In general, *feeding* an antenna is more complicated than simply connecting the amplifier's positive and negative terminals to the antenna's terminals. A  $50\Omega$  characteristic impedance is often used in RF systems. Since each antenna has a unique *input impedance* which is generally different from this value, it must be *matched* appropriately for optimal performance. A few well-known techniques for a number of the antennas in Section 2.3.1 are reviewed below.

#### **General**

A general, antenna-agnostic narrow-band technique for antenna impedance matching is to employ a "lumped element" matching circuit consisting mainly of inductors and capacitors. The most common example of this is an L-section, with exactly one capacitor and inductor.

#### **Half-Wavelength Dipole**

A half-wavelength dipole antenna has an input impedance of around  $73\Omega$ , varying only due to the wire diameter used. A common method to reduce this impedance to  $50\Omega$  is simply to reduce the length of the dipole. In this case, a  $50\Omega$  match occurs from  $0.42\lambda$  to  $0.44\lambda$ . [17]

#### **Helical**

The input impedance of a helical antenna varies between 100 and 200 ohms. A common method to reduce this impedance is for the first quarter turn of the helix to be in the form of a conductive strip, and for the *pitch angle* of this section to be close to zero [17]. The height above the ground plane can then be varied to match the antenna appropriately, with the following equation approximately providing an approximate  $50\Omega$  match [17]:

$$h = \frac{w}{\frac{377}{\sqrt{\epsilon_r} Z_0}} - 2$$

### 2.3.3 Summary

The following table presents a general summary of the investigated antennas. A qualitative comparison of the results have been presented from general consensus in literature to aid in the design phase. Note that a *narrow* beamwidth general corresponds to a *uni-directional* antenna (and wide for omni-directional) and therefore this characteristic has not been included in the table. However, a graph of antenna beamwidth as a function of gain has been included in Appendix B.1 as a reference.

Type	Gain (dBi)	Beamwidth	Bandwidth	Size	Polarization
0.5λ Dipole	2.15	Omni-directional	Medium	Medium	Linear
Monopole	5.15	Omni-directional	Small	Small	Linear
Helical	< 20	Either	Large (50 - 60%)	Small-Medium	Circular
Microstrip	< 10	Either	Small-Medium	Small	Either
Yagi-Uda	< 40	Uni-directional	Small	Large	Linear

**Table 2.1:** Qualitative Comparison of Antenna Characteristics [8]

## 2.4 Telecommunication

### 2.4.1 Modulation Techniques

The *modulation* technique used over a communication link refers to the method used to encode analog or digital information into an electrical voltage. ASK, FSK, PSK, and QAM are the most common techniques [20] [21]:

- *Amplitude Shift Keying* (ASK). This technique modulates the amplitude of the voltage to represent various bit levels.
- *Frequency Shift Keying* (FSK). This method changes the frequency of the signal to represent various signal levels. Commonly, *Gaussian-FSK* (GFSK) is used, which implements a smoothing filter. This decreased the bandwidth for similar throughput, making it comparable to the following techniques.
- *Phase Shift Keying* (PSK). This is often seen as a variation of FSK, where the phase of the signal is varied instead of the frequency. It requires complex synchronisation, and has lower spectral efficiency compared to QAM.
- *Quadrature Amplitude Modulation* (QAM). This method modulates both the amplitude and phase of a signal, allowing for a large number of signal levels. It has very high spectral efficiency, and is commonly used for high cost, high throughput systems.

*LoRa* ("Long-Range") modulation is a relatively new technique. It makes use of frequency-varying "chirps" to modulate the incoming signal. It has been seen to drastically increase range capacity, at the expense of greater bandwidth requirements [22]. Its practical use has also been demonstrated in an existing CubeSat system [23].

## 2.4.2 Link Budget

For any communication system, a "link-level" design or *link budget* should be conducted. The goal of this design step is to determine the power requirements of the communication system, taking into account transmitter power, antenna characteristics, receiver sensitivity, modulation technique, and any attenuation involved. A number of the attenuation affects which may be taken into account in a satellite link budget include [24]:

- Cable loss
- Amplifier-antenna mismatch
- Free-space path losses
- Absorption losses due to clouds, rain etc.
- *Polarization* mismatch due to antennas not being aligned
- *Scintillation* effects due to changes in the air's refractive index
- The effect of varying *elevation angles*

Further, it is recommended to include a minimum margin or *fade margin* of at least 3 dB for low frequency links [25], up to 10 dB for links that require more up-time [26], and around 20 dB for mission critical links.

## 2.4.3 Protocols

A few link-layer and network-layer protocols already exist that facilitate nano-satellite applications. The CubeSat Space Protocol (CSP) [27] is a fully-fledged network layer protocol for CubeSat embedded systems. It allows for all devices in the satellite ecosystem (satellite modules, the ground station, a control computer etc.) to communicate "directly" with each other via *packet forwarding*. It relies on various link and network -layer protocols, including KISS, I2C and CCSDS (*Consultative Committee for Space Data Systems*).

# 3. System Design

## 3.1 High-Level System

A complete high-level system block diagram illustrating the system-level decisions is shown in Figure 3.1. Note that the yellow blocks are external (i.e. assumed to be available already).

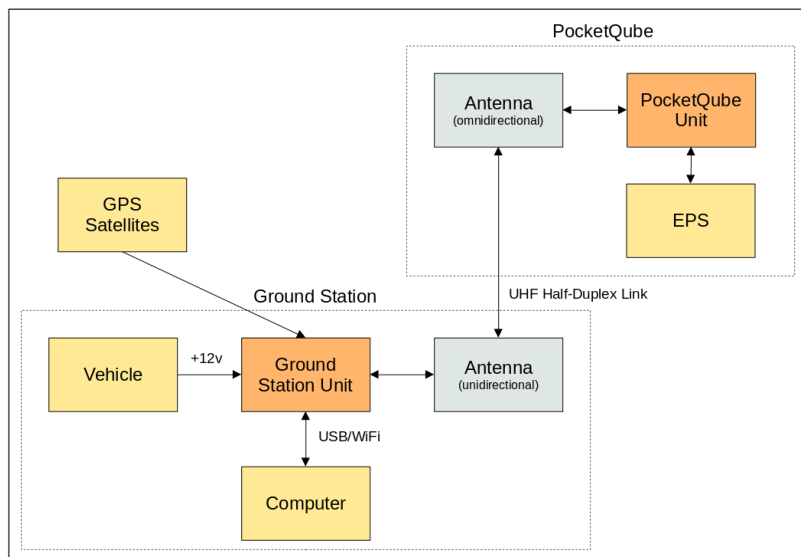


**Figure 3.1:** High-Level System Diagram

### 3.1.1 Methodology

Since a large number of sub-systems are required on the ground-station, either IC *modules* or simple *reference designs* will form the basic building blocks of the system. Only if no modules or designs are found to meet the system requirements, will a more custom solution be developed. The ground station will be powered via +12V from a nearby vehicle, and the PocketQube will be powered from an on-board EPS (another PQ unit). Both sub-systems should be designed such that testing without a vehicle/EPS is also possible.

### 3.1.2 Tracking

Further research shows that trajectory predictions for both the landing area and the dynamic altitude of a balloon can be up to 15-20 km inaccurate for a standard 2 hour flight [28]. For

the worst case, this is a total inaccuracy of  $\sqrt{20^2 + 20^2} = 28$  km. For the designed range of 120 km, this results in an angle inaccuracy of  $360 \times \frac{28}{2\pi \times 120} \approx 14^\circ$ .

An antenna with a beamwidth of double this inaccuracy is therefore required. A Yagi-Uda antenna with a beamwidth of around  $28^\circ$  has a gain of around 17 dBi, as seen in Figure B.1. Using a common Si4311 FSK receiver's sensitivity of -104 dBm, an initial link budget can be estimated. Assuming 100 mW (20 dB) transmit power, the full 22 dBi gain, and 127 dB path loss attenuation loss at 115 km, a 10 dB link margin is obtained.

Since the above link budget clearly indicates that open-loop tracking is feasible, it is decided to focus on this as the main tracking method. The ground station therefore requires at least a GPS connection; a means of determining true north (such as a magnetometer); and a means of uploading path data. The path data will be uploaded to the ground station via USB from a system computer. If time allows, direct GPS tracking will then be added as a method of "closing the loop", and to improve pointing accuracy.

### 3.1.3 Custom Link

A half-duplex link will be designed. This is decided on due to the nature of the link itself (i.e. either downlink "telemetry" or a simple command-response "telecommand" pattern) and due to the added complexity that full-duplex would require (i.e. a dual frequency system).

For the given flight path, a goal of at least 9600 downlink baud rate will be designed for at the 120 km range, with LoRa being explored as the main modulation technique. This is chosen due to the high sensitivity it offers (which will help alleviate the need for a large, high-gain antenna), as well as the link speed it offers for reasonable bandwidth ( $< 500$  kHz). GFSK will be considered as a backup option, since it is well-established in literature. The 433 MHz amateur band (430 to 440 MHz) will be utilized.

## 3.2 Ground Station

### 3.2.1 Power

The power section consists of two linear regulators, as well as a boost converter. Since the existing motors are ideally powered from +24V, a boost converter will be used to step up the voltage from a car battery voltage of +12V. Further, +5V and +3V3 regulators will be included to power both the MCU and any other ICs. Linear regulators were selected, due to their simplicity, as well as the lack of any specific system-wide efficiency requirements.

### 3.2.2 Communication

The communication section consists of the main antenna, as well as the RF circuitry and connectors. The *RF Switch/Connector* is provided to allow the antenna to be shared between the custom and radiosonde communication links. Initially, a connector will be used for

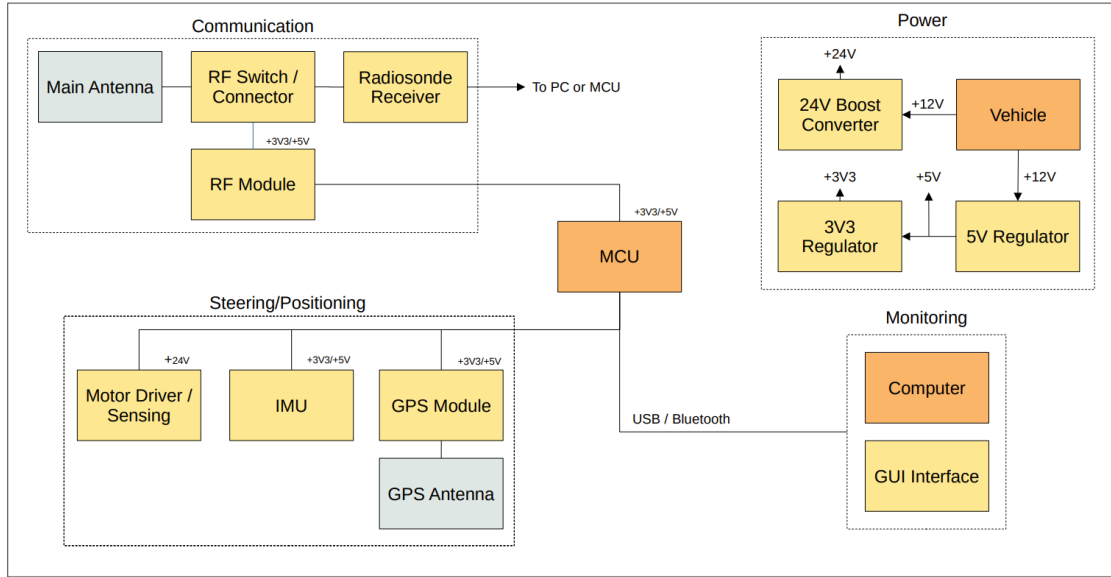


**Figure 3.2:** Groud Station System Diagram

prototyping. If time allows, a dedicated RF switch could be included, which will allow for the MCU to control the antenna connection. The radiosonde will either connect to the PC (e.g. if an SDR dongle is used) or to the MCU (if a dedicated receiver is used).

### 3.2.3 Steering and Positioning

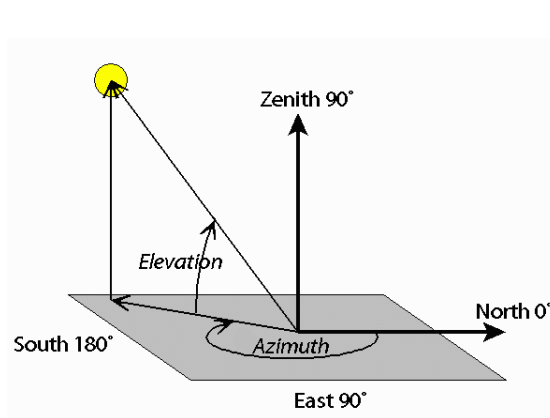


**Figure 3.3:** Azimuthal and Elevation Vi-  
sualization [6]

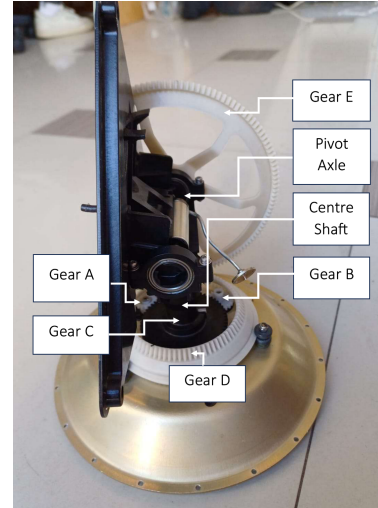


**Figure 3.4:** The Existing Antenna Mount

Generally, the orientation of a ground station's antenna is described by both an azimuthal and an elevation angle, as in Figure 3.3. The existing two-axis antenna mount is shown in Figure 3.4. Since the antenna platform moves relative to the base (where the PCB is mounted), this relative angle needs to be known. Two options to do this are considered:

1. *Open-loop.* The base's absolute orientation is measured/known, and the platform's relative orientation is calculated/looked up based on the stepper motor positions.

2. *Closed-loop*. The platform's absolute orientation is measured in real-time, and this information is fed back into the motor's control system to point the platform correctly.

Since stepper motors are already included, *open-loop* method will be considered, however the closed loop method may be implemented if this method is found to lack accuracy, or the motor locations are found to be unpredictable. In this case, an inertial measurement unit (IMU), which typically includes an accelerometer and gyroscope, will be used.

### 3.2.4 Monitoring

A laptop will be used with a simple Graphical User Application (GUI) allowing the user to:

- Send commands to the ground station and/or satellite.
- Read telemetry of the satellite.
- Control the ground station orientation e.g. performing motor calibration etc.
- Set communication parameters e.g. output power and modulation parameters.
- Monitor communication link performance.

## 3.3 PocketQube Unit

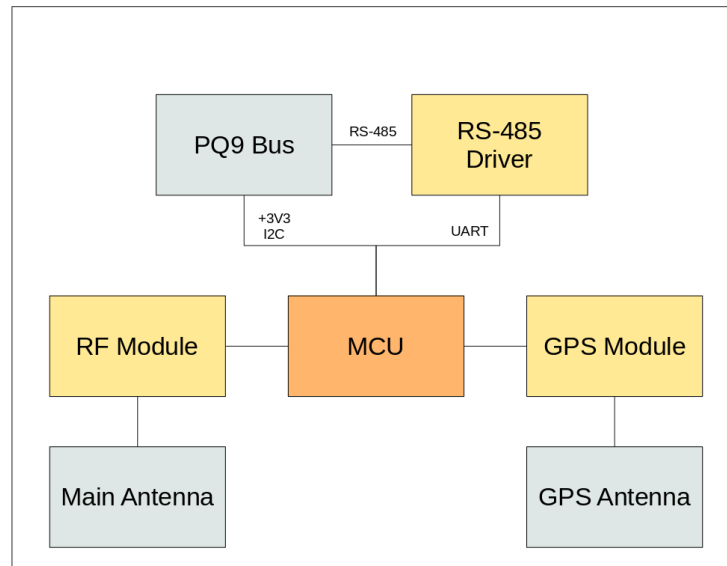


**Figure 3.5:** PocketQube Unit System Diagram

A block diagram of the system components for the PocketQube unit is shown in Figure 3.5. This unit is relatively simple in comparison to the ground station. The unit consists of an RF section, and a GPS section. The system will be powered via the +3V3 on the PocketQube bus. An integrated GPS module, as well as RF module, should be included. Further, an RS-485 line transceiver should be included to cater for the RS-485 protocol, which will likely connect to the MCU via UART.

# 4. Detailed Design

## 4.1 Component Selection

The first step in the detailed design process is to select components for the various sub-systems. Components for both the ground station and PQ unit will be selected in one step, due to the overlapping research involved. Through-hole components and breakout boards will mostly be used for the ground station, and surface mount components for the PQ unit.

The ground station has a number components which will be used without modification. The existing stepper motors draw 0.50 A and allow for up to 0.5 N · m of torque [29]. The ground station also includes a small zero-sensing circuit for the azimuthal direction, which integrates a *H22A* optical switch [30] and a low-pass filter.

### 4.1.1 GPS

The same GPS will be selected for both the ground station and PQ unit to simplify development. A small one degree pointing accuracy will be designed for, since each degree of inaccuracy from the GPS for open-loop tracking requires the antenna's beamwidth to be one degree larger. A distance of 120 km therefore results in a required accuracy of  $2 \times 120000 \times \pi \times \frac{1}{360} \approx 2 \text{ km}$ .

The NEO line of GPS modules from *u-blox* (e.g. the *NEO-6M*) are very commonly used, and are quoted to have a 2.5 m accuracy, however there was limited availability of these modules from local suppliers at the time of ordering. Other modules with similar specifications were therefore considered, such as the *ATGM336H* and the *ATGM332D*. Since both of these advertise 2.5 m accuracy, active antenna support, and current consumption less than 100 mA, the *ATGM332D-5N31* was chosen for its lower price.

### 4.1.2 IMU

To determine absolute azimuthal rotation, the ground station (either the base or the platform) should either be manually positioned to face north, or a magnetometer may be used. Further, to allow for further flexibility, the ground station may be mounted and tilted on a tripod. In this case, an inertial measurement unit (IMU) may be needed to determine the mount's absolute rotation.

As seen in Section 4.1.1, low accuracy is required. A low-accuracy IMU will therefore be

included, with an accelerometer and magnetometer. The *BNO055* is a 9-axis IMU which integrates an ARM Cortex-M0 for signal processing. It operates at 100 Hz, has 0.3  $\mu\text{T}$  magnetic field resolution, and around 16 bit sensors. It is, however, very expensive (around R800). The *MPU-9250*, and the *MPU* line of IMU's are seen as cheaper alternatives. Since the ground station's mount will not be moving, only a low-accuracy accelerometer is assumed to be adequate for orientation, as research indicates. The *MPU-9250* also has a 16-bit accelerometer, and only a slightly lower magnetic field accuracy (0.6  $\mu\text{T}$ ), and therefore was selected..

### 4.1.3 RF Module

The transciever type for both the custom and radiosonde link needs to be considered. There are a few options in this regard, listed from more to less specialized:

- Fully custom design. Here, all components are discretely designed using transistors, MCUs etc. This option is listed for completeness, but is out of the scope of this project.
- Front-End Module (FEM). For this option, the FEM provides filters, a low-noise amplifier (LNA), antenna matching, and down-conversion. Then, a controller (e.g. FPGA or MCU) needs to be designed to perform modulation/demodulation functionality (the *modem*) and interface with the FEM.
- Dedicated Transciever. A transciever provides both the FEM functionality and the software modulation, however still requires RF techniques for matching, as well as an additional RF shield.
- Dedicated module. For this option, all functionality is provided in a dedicated module, with a simple antenna connection/pin and MCU interface. This method has little flexibility, since all matching is done internally, and the frequency band is therefore constrained, however provides highest ease-of-use.
- Software-defined radio (SDR). This is the most general-purpose option, but does not exercise the highest performance. It is often directly connected to a computer.

### Custom Communication

For the custom link, a dedicated LoRa module will be used. Most of these modules include GFSK as a built-in alternative, which makes them the ideal choice. All LoRa ICs are based on *Semtech* chipsets due to the company's patent on the technology. Although dedicated transceivers are available, these require special RF considerations to be made, as discussed, and therefore a module will be utilized to ease development.

Unfortunately, few modules exist that allow for reception both in the 405 MHz and the 433 MHz bands, even though some of the chipset are capable of this. Table 4.1 contrasts the two most common modules in the 433 MHz LoRa band which offer this feature, both based

on the SX1278 chipset. If time allows, a more custom module can be designed. The RA-02 is ultimately selected due to its availability and cost.

Name	RX Sensitivity	TX Sensitivity	Frequency
RA-02	-141 dBm	+18 dBm	410 to 525 MHz
RFM98	-148 dBm	+20 dBm	410 to 525 MHz

**Table 4.1:** Comparison of two LoRa modules

## Radiosonde Communication

Since the radiosonde communication protocol will require some investigation, and the exact encoding and GFSK parameters are unknown, software-defined radio (SDR) will be utilized to allow for flexibility. Universal Radio Hacker (URH) (<https://github.com/jopohl/urh>) and GNU-Radio (<https://www.gnuradio.org/>) are both free software solutions available to investigate wireless protocols using an SDR. The “RTL-SDR” USB dongle is considered the standard, low-cost solution for this, and is therefore selected for this project. If time allows, however, a more dedicated transceiver could be included, along with an RF switch, to remove the need for an additional USB connection.

### 4.1.4 Stepper Motor Driver

The original PCB of the previous antenna mount system contained two A3972 ICs to drive the stepper motors. Although these could be de-soldered and used, it is favourable to use a newer supported IC with better capabilities, and for easy replacement in case of damage. From the driver and motor datasheets, the following specifications are realized:

- Dual DMOS Full-Bridge Output Configuration
- Bipolar PWM current control
- Micro-stepping (for smoother stepping)
- 0.5A, 24V

Very few drivers fit these exact specifications. The *A4970* is considered the follow-up version of the *A3972*, however is not available in a single pack or locally. The *L6219* driver is found to match these specifications and will be selected due to availability.

### 4.1.5 Power

Both a 3.3V regulator and 5V regulator will be needed for the ground station power distribution. The LD1117V33C and L7805CP are chosen respectively due to their availability. A boost converter will also be needed to achieve the 24V motor drive voltage. Since each stepper

motor will draw around 0.5 A per coil, the converter should support 2 A at its 12 V input. A breakout board based on the XL6009 IC will be used, which meets this specification.

### 4.1.6 Microcontroller

A general-purpose MCU will be needed both on the GS and the PQ. The three most popular frameworks/MCU types for this are the ESP32, Arduino, and STM32.

The *ESP32-WROOM-32* is a commonly available ESP32 variant which has 32 GPIO pins, of which several can be used as an ADC input, SPI or I2C interface. This means that there are 23x GPIO available - enough for this project. Further, the ESP32 has the added benefit of WiFi and Bluetooth connectivity, which may allow "smart" features to be added to either devices in the future. The *ATMEGA328PB* is an MCU commonly used in small Arduino boards. It, however, has fewer pins than the ESP, is an 8-bit MCU, and has only 32 KB of flash memory.. It does, however, allow a supply voltage of as low as 1.8V, and has very low current consumption. Finally, the common *STM32F411* MCU is a high-performance, ARM-Cortex board advertised to have highly accurate ADCs and up to 81 GPIOs.

Since the processing requirements for this project are not very high, and the ESP32 is a relatively high-performance MCU which satisfies the pin requirements, with added "smart" capabilities, it will be selected for the GS. For the PQ unit, the ATMEGA328PB will be used, due to its exceptionally low current consumption, and many fewer pins being needed for the PQ unit.

### 4.1.7 RS-485 Driver

Most RS-485 drivers come in a common 8-pin form factor. Due to having very little requirements (i.e. short range communication, no speed specifications) the *SN75179BDR* is selected due to its availability.

## 4.2 Ground Station PCB

### 4.2.1 Circuit Design

Since the ground station mainly consists of various sub-systems and components, "typical application" circuits found in component datasheets were mostly employed. The final schematic is found in Appendix C.1.

#### Power

Current calculations should be done to ensure that the voltage regulators and the boost converters can provide enough power where necessary. A car socket can supply up to 10 A at

+12 V (i.e. 120 W). The supply voltage, current consumption, and power consumption of the various system components is listed in Table 4.2. In all cases, maximum current is provided.

Component	Voltage	Current	Power
Motors	24 V	0.5 A (x4)	48 W
ESP32 Dev Board	5 V	120 mA	660 mW
RA-02	3.3 V	100 mA	330 mW
ATGM332D-5N31	3.3 V	25 mA	82.5 mW
MPU-9250	3.3 V	3.7 mA	12.21 mW

**Table 4.2:** Ground Station Component Power Consumption

Therefore, maximum consumption - even at full motor current draw - is only 50 W, and will not place heavy load on the car socket battery supply. The 3.3 V regulator should be capable of supplying around 130 mA, and the 5 V regulator around  $120 \text{ mA} + 130 \text{ mA} = 250 \text{ mA}$ . The LD1117CV can supply up to 800 mA, and the L7805CP up to 1.5 A, meaning the limitations are met.

The power section also includes selector jumpers to isolate it from the rest of the board. In this way, if a component is damaged during implementation, or if the power section is found to not be working, external power can be supplied appropriately.

## Motor Drivers

The L6219 drivers require a reference voltage to set the maximum current. According to the datasheet [31], a peak current of  $I_{max} = 10 \times \frac{V_{ref}}{R_s}$  in mA is used. Since the recommended value of  $R_s = 1 \Omega$  is being used,  $I_{max} = 10 \times V_{ref}$  mA. Since the motors allow up to 500 mA per winding, a current value of  $I_{max} = 475$  mA is chosen to prevent damaging the motors. Therefore,  $V_{ref} = 4.75$  V. This can be implemented with a voltage divider. Setting the upper resistor  $R_1 = 1 \text{ k}\Omega$  results in  $R_2 \approx 20 \text{ k}\Omega$ , as shown in the schematic. The disadvantage of this method is that the maximum current cannot be controlled dynamically. The reference voltage can be replaced with a DAC from the MCU if more control is required.

## Connectors

The RA-02 RF module states that not all data pins are necessary. Further, it was assumed that there may be some errors in the original design. A male header was therefore provided for unused GPIO pins, to allow for flexibility once the PCB was manufactured.

### 4.2.2 PCB Design

A 2-layer stackup was decided on, so that the board could be manufactured in-house early on in the project (as the in-house PCB machine has a 2-layer limitation). The final PCB was designed in KiCAD. A screenshot of the front layer is shown in Appendix C.3. The board

was designed to be compatible with the mount with the relevant mounting holes and motor cut-outs. Female headers were used for most of the modules, since development boards were being used. Two PCB pours were exposed below the voltage regulators to act as a heat sink for added heat dissipation.

## 4.3 PocketQube Unit PCB

### 4.3.1 Circuit Design

To design the PocketQube PCB, since no development boards were used, the Arduino Nano schematic in [32] was consulted as a reference design. It was decided to simply expose the relevant pins needed to flash the MCU, instead of integrating a USB connection directly, however this could be added for future iterations. The final circuit schematic can be found in Appendix C.2.

#### Power

The maximum power consumptions of the on-board components is found in Table 4.3. A total maximum power consumption of around 600 mW is calculated. This equates to around 200 mA draw for a 3.7 V LiPo battery. To achieve the 3 hour specification, a capacity of 600 mAh is therefore required. A larger 2000 mAh battery was used for development, due to the added convenience, as well as the fact that it would allow for location of the payload after the balloon has landed up to 7 hours later.

Component	Current	Power (@ 3V3)
ATmega328	12 mA	39.6 mW
RA-02	100 mA	330 mW
ATGM332D-5N31	25 mA	82.5 mW
SN75179B	57 mA	188 mW

**Table 4.3:** PocketQube Unit Component Power Consumption

#### RF and GPS Modules

Since the RA-02 RF module has a u.FL connector onboard, no considerations need to be taken with respect to impedance matching at the interface between the module and the antenna feed. However, the ATGM332D GPS module directly exposes its RF input via one of its SMD pins, meaning impedance matching may need to be done. The higher L1 GPS band operates around 1575.42 MHz, which is a wavelength of  $\frac{3e8}{1575.42e6} = 190$  mm. The "critical length" (the length at which reflections can be ignored) is therefore around 19 mm. Since this is relatively large, if the trace length between the module and antenna interface is kept shorter than this, impedance matching will not be necessary.

### 4.3.2 PCB Design

It was decided to use a 2-layer board, due to the low component count. Although the impedance matching is not necessary for the GPS module, it is still desirable to control the trace impedance as much as possible. However, a 50-ohm trace on a 2-layer board is around 2.8 mm (determined using a microstrip impedance calculator), which is much larger than the pad sizes of the GPS module. Therefore, the trace was simply made as wide and as short as possible. The final PCB was designed to conform to the PocketQube standard, as shown in Figures 4.1 and 4.2.

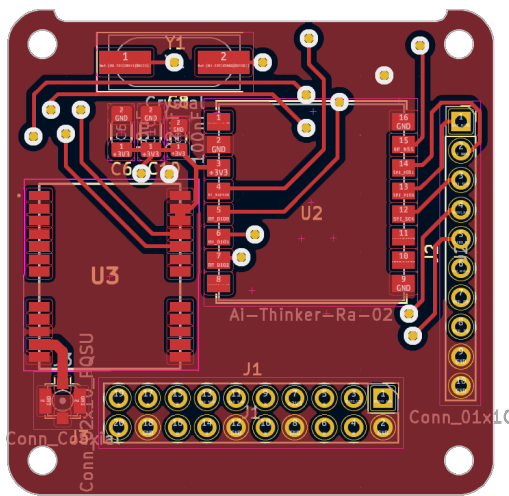


**Figure 4.1:** PocketQube Unit PCB Design (Front)

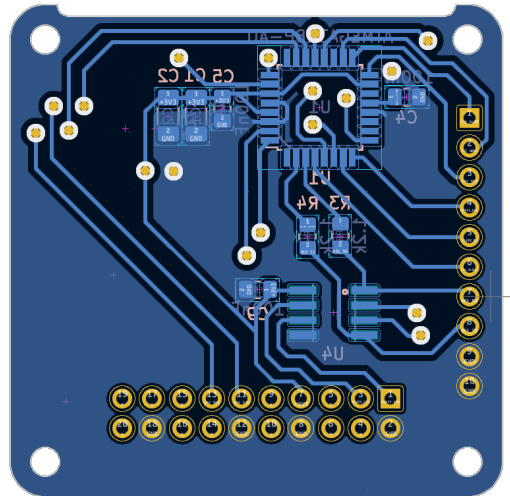


**Figure 4.2:** PocketQube Unit PCB Design (Back)

## 4.4 Link Budget

The link budget should now be estimated, and initial considerations for the ground station's base location should be made, as this location will affect the range of elevation angles to accomodate, the distance to the horizon, and the free-space path loss.

Signal Hill in Cape Town is a viable location for the ground station and is easily accessible. At its distance of 114 km, however, one would need to be at a height of 950 m due to the distance to the horizon. Therefore, the balloon would only be visible at an altitude of 600 m (from Signal Hill's 350 m height). A maximum elevation angle of  $16.72^\circ$  at 30 km altitude above Worcester should be considered.

The *receiver sensitivity* is a value which denotes the minimum power level required at the receiver for successful communication. Depending on set parameters, the SX1278 quotes varying receiver sensitivity values. Notable configurations are listed in Table 4.4.

Description	Modulation	Parameters	Bit Rate	Sensitivity
Maximum Bit Rate	GFSK	62.5 kHz	250 000 bps	-92 dBm
High Bit Rate	GFSK	40 kHz	38400 bps	-109 dBm
Target Bit Rate ( $\approx 9600$ bps)	GFSK	5 kHz	4800 bps	-115 dBm
-	LoRa	500 kHz, SF 8	10417 bps	-119 dBm
Maximum Sensitivity	LoRa	62.5 kHz, SF 12	24 bps	-147 dBm

**Table 4.4:** Notable SX1278 Configurations

An online path loss calculator was used to calculate attenuation due to distance, and the Python tool *link budget* was used to calculate atmospheric losses. All values were based on both the RA-02 and the SX1278 chip specifications, as well as half-wavelength dipoles as antennas, an impedance mismatch loss of 0.5 dB (around -10 dB return loss), and a maximum transmitter power setting (18 dBm).

Transmitter Power	18 dBm
Mismatch Loss	(0.5 dB)
Transmission Line Loss	(1 dB)
Antenna Gain	2.15 dB
<b>EIRP</b>	<b>18.65 dBm</b>

**Table 4.5:** Link Budget - Satellite

Free space path loss (114 km)	126.3 dB
Atmospheric loss	0.22 dB
Scintillation loss	0.37 dB
Polarization Mismatch	3 dB
<b>Total Loss</b>	<b>129.89 dB</b>

**Table 4.6:** Link Budget - Channel

Antenna Gain	2.15 dBi
Mismatch Loss	(0.5 dB)
Transmission Line Loss	(1 dB)
Receiver Sensitivity	119 dBm
<b>GS Sensitivity</b>	<b>119.65 dBm</b>

**Table 4.7:** Link Budget - Ground Station

The LoRa "target bit rate" sensitivity value of -119 dBm is used in the above calculations. The final link budget therefore results in  $18.65 \text{ dBm} - 129.89 \text{ dB} + 119.65 \text{ dBm} = 8.41 \text{ dB}$  of link margin. Although this is theoretically adequate (above the 3 dB recommendation), there are a few considerations to be made:

- If a higher bit rate is required, e.g. 38.4 kbps, then the margin drops to -2.6 dB.
- If a longer range is required (e.g. for future projects), free space path loss will drastically increase. For example, for a 250 km range, the loss becomes 133 dB, meaning the margin drops to only 1.1 dB.

To achieve the 10 dB recommended link margin, an antenna with at least 2.59 dBi additional gain (i.e. 4.74 dBi gain total) should be designed for the ground station. Then, if necessary, the 20 dB recommendation can be reached by lowering the LoRa spreading factor (SF) to support any "mission critical" requirements. Practically, this "mission critical" setting could be initialized as the system's "startup" state, until a connection is made, where the SF can then be changed to an appropriate value.

## 4.5 Ground Station Antenna

### 4.5.1 Mechanical Considerations

The existing antenna mount is shown in Figure 3.4. Azimuthal and elevation stepper motors are connected directly through Gear A and B respectively. Gear A rotates the centre shaft to provide azimuthal steering, whereas Gear B rotates through Gear D and E to allow a change in elevation. The specifications in Table 4.8 were realized.

Component	Specification
Motor	200 full steps (per 360 degrees)
Gear A	15 teeth
Gear B	20 teeth
Gear C	60 teeth
Gear D	92 inner teeth, 80 outer teeth
Gear E	140 teeth (equivalent)

**Table 4.8:** Mount Gear and Motor Specifications

The black plastic platform is triangular and has three mounting holes. The new ground station's antenna should therefore be mounted onto this platform. It is important to consider the forces/torques involved, as well as the stepper motor holding torques, in order to determine the maximum weight and acceptable form factor of the new antenna.

The azimuthal motor need not be considered, as all torques from the mount to its base are perpendicular to the central shaft, meaning it would only need to overcome static frictional

forces to rotate the antenna, which are assumed to be negligible. The holding torque of the elevation motor, however, will constrain the antenna design. The holding torque of each motor is 0.25 Nm. The gearing ratio resulting from Gears B, D and E, results in an around 8x torque increase. This provides a holding torque of around 2 Nm at the pivot axle.

The centre of gravity of the antenna, as well as its weight, will affect the motor's ability to hold it in place. The horizontal distance between the pivot axle and the mount in the upright position is measured to be 40mm. Therefore, in the worst-case (when the mount is upright as in Figure 3.4) a planar antenna could weigh up to  $\frac{2}{(9.8 \times 0.04)} = 5.1$  kg. In general, the "mass-distance" product of the antenna (mass times distance of centre of gravity from mount) should not be more than 0.2 kg · m. This should be strongly considered if a longer antenna is desired.

The physical dimensions of the antenna's ground plane is also constrained. A circular ground plane may make contact with the mount's base at low elevation angles (assuming the ground station itself is raised above the ground). When the mount is resting, this constraint is imposed when the ground plane first makes contact with the mount's base. For a circular ground plane, this is around 360 mm diameter at an elevation angle of around 35 degrees.

## 4.5.2 Theoretical Design

As discussed, the antenna should be capable of receiving from both the 405 MHz radiosonde link, as well as the custom LoRa-based link in the amateur radio band of 430 to 440 MHz. A helical antenna is suggested, for the following reasons:

- Ability to increase gain arbitrarily by increasing the number of windings
- High fractional bandwidth of 56%, which may allow for a smaller antenna than other antenna types
- Ease of manufacture

The centre frequency  $f_c$  of the antenna should first be selected. With a fractional bandwidth of 56%, the inequality  $f_c \times (1 - \frac{0.56}{2}) < 405$  MHz must hold. This gives an upper bound on the centre frequency of 562.5 MHz. A minimum ground plane diameter of no smaller than  $0.5\lambda$  is recommended in [17], and  $0.75\lambda$  in [33]. It is, however, probable that a ground plane as small as  $0.5\lambda$  will adversely affect the radiation pattern near the end of the specified bandwidth.

Assuming the larger ground plane recommendation, the resulting ground plane diameter is  $0.75 \times \frac{3e8}{562.5e6} = 400$  mm, which is larger than the mechanical size constraint. Nevertheless,  $f_c = 550$  MHz is chosen as the initial centre frequency for simulations. the ground plane will then be decreased in size appropriately (towards  $G_\lambda = 0.5$  i.e. 270 mm) and the results observed.

The design parameters for a helical antenna are  $f_c$  (centre frequency),  $n$  (number of turns),  $S$  (the spacing between turns),  $C$  (the circumference) and  $G$  (the ground plane diameter).

Design formulae are provided in [17], and have been modified below to use relative values instead of absolute ones (i.e.  $S_\lambda$  and  $C_\lambda$  instead of  $S$  and  $C$ ). Directivity, in dBi, is given by:

$$D_0 = 10 \log(15 \cdot nS_\lambda \cdot C_\lambda)$$

$C_\lambda$  is typically kept at 1.0, meaning the circumference is equal to the operating wavelength. As mentioned, a gain of around 5 dBi is required. However, a 3 dB bandwidth drop is estimated nearer to 400 MHz since it is the edge of the operating band. Further, the effect of a smaller ground plane will likely decrease performance by an estimated minimum of at least 1 dB. Therefore, a centre-frequency gain greater than 8 dBi will be designed for. This will also move the system towards the 20 dBi link margin. For this gain, the  $nS_\lambda$  product should equal around 0.45. Although the optimal value for  $S_\lambda$  is 0.23 [17], smaller values have been quoted to work [18] and are mechanically easier to construct. Therefore,  $S_\lambda = 0.15$  is chosen, and finally,  $n \geq 3$ .

### 4.5.3 Simulation Design

Simulation of a helical antenna is well documented in literature, and therefore the parameters can be varied iteratively and integrated into the antenna design process. For this project, FEKO software is used. An initial model with the above parameters, a large ground plane ( $G_\lambda \approx 1.0$ ), and a wire diameter of 2.5 mm (chosen due to availability) is simulated. The resulting radiation pattern at the centre frequency of  $f = 550$  MHz is shown in Figure 4.3, with a maximum gain of around 9.5 dBi.

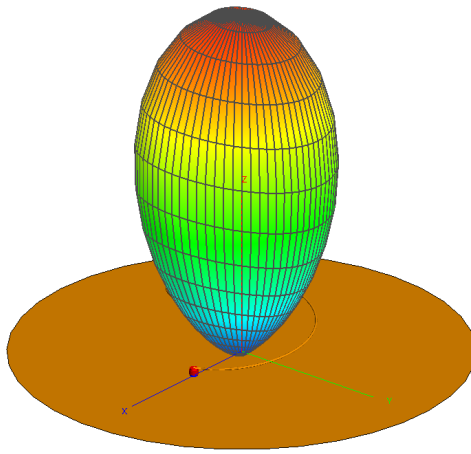


**Figure 4.3:** Initial Simulated Helical Antenna Radiation Pattern ( $f = 550$  MHz)

Most of the follow-up design is conducted around the lower frequency of  $f = 405$  MHz. The radiation patterns for  $G_\lambda = 0.5$  and  $G_\lambda = 0.7$  ( $G = 273$  mm and  $G = 382$  mm) are shown in Figures 4.4 and 4.5 respectively. It is clear that the recommended value of  $G_\lambda = 0.5$  from [17] will not work near this lower frequency, as shown by the morphed radiation pattern. The pattern is found to be acceptable at around  $G_\lambda = 0.7$ . However, after analysing the

input impedance for this ground plane size (shown in Figure 4.6) it is clear that broadband matching would be difficult, due to the drastic change in impedance near the lower end of the spectrum.

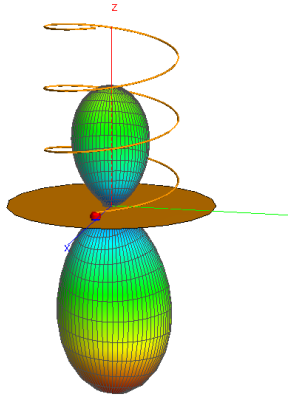


**Figure 4.4:** Simulated Helical Antenna Pattern at  $f = 405$  MHz ( $f_c = 550$  MHz,  $G_\lambda = 0.5$ )

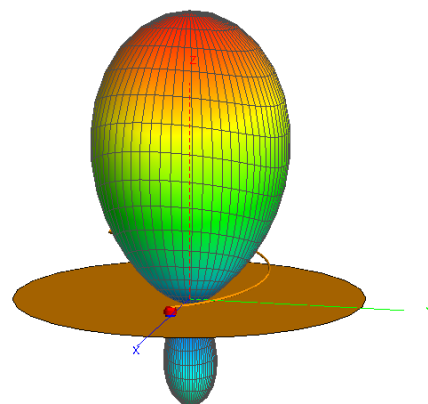


**Figure 4.5:** Simulated Helical Antenna Pattern at  $f = 405$  MHz ( $f_c = 550$  MHz,  $G_\lambda = 0.7$ )

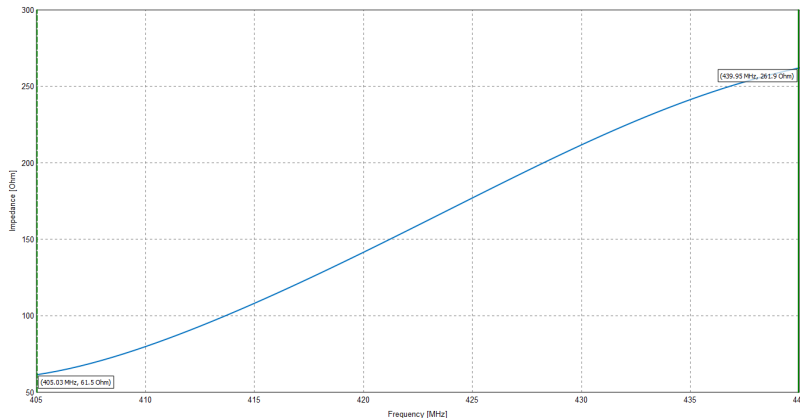


**Figure 4.6:** Simulated Helical Antenna Input Impedance ( $f_c = 550$  MHz,  $G_\lambda = 0.7$ )

In order to ease matching, a lower centre frequency should ideally be used, to move the input impedance at 405 MHz and at 433 MHz closer together. This will, however, require either a larger ground plane, or a cupped ground plane (discussed further on). Unfortunately, FEKO does not allow for an optimisation goal that depends on two frequencies. Therefore, an iterative approach was used to find the centre frequency which minimizes the difference between the two impedances. The resulting centre frequency was found to be around  $f_c = 510$  MHz at  $G_\lambda = 0.6$  ( $\approx 350$  mm), with a resultant input impedance close to  $250\Omega$ , as shown in Figure 4.7.

Since the mount can support a larger weight than the 3 turn coil, it was decided to experiment with larger a turn count (i.e.  $n = 4$ ), both for increased directivity/performance, and to potentially cater for manufacturing imperfections, such as a thin aluminium foil ground plane, and any diversions from the ideal helical shape. It was found that, for small ground

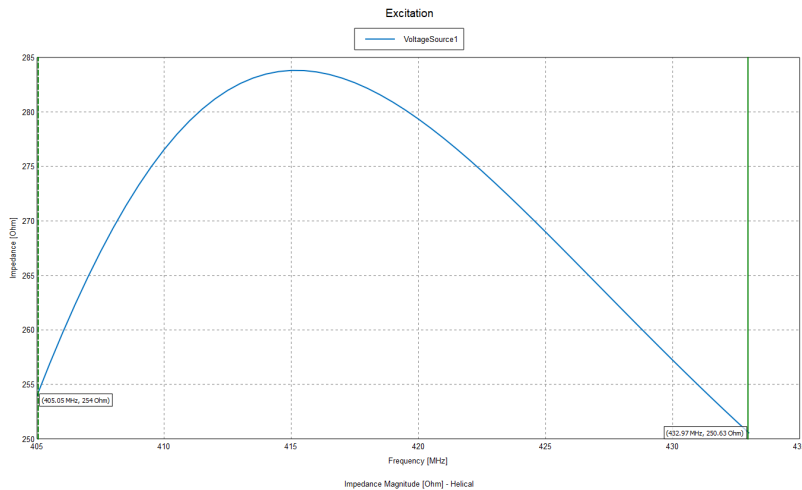


**Figure 4.7:** Simulated Helical Antenna Input Impedance ( $f_c = 510\text{ MHz}$ ,  $G_\lambda = 0.6$ )

plane diameters, as the number of turns increased, the radiation pattern for  $f = 405\text{ MHz}$  was negatively affected. This is intuitive when referring to image theory, as the non-idealities due to the finitely-sized ground plane become more apparent as distance to the plane increases. It should be noted that the pattern at  $f = 433\text{ MHz}$  was not as adversely affected.

The ground plane was therefore cupped, and the results observed. At  $G_\lambda = 0.6$ , a cup height equal to 1 helical turn was found to greatly improve the radiation pattern. This is shown in Figures 4.8 and 4.9. The gain, however, was not as drastically affected.

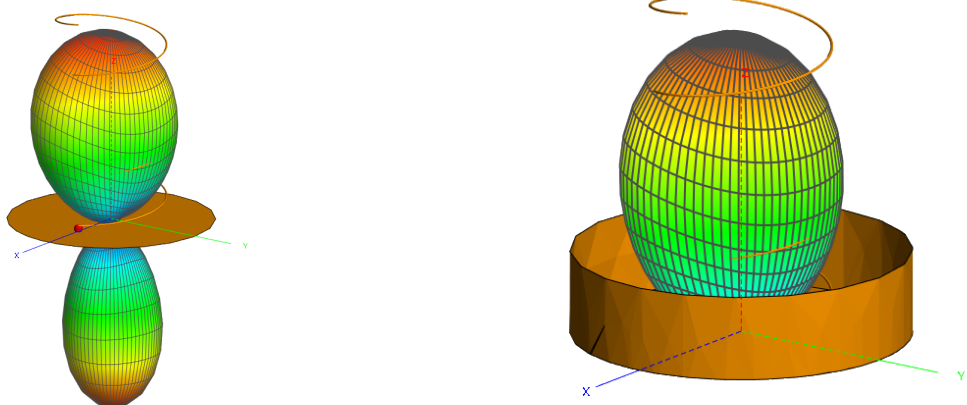


**Figure 4.8:** Simulated Helical Antenna Pattern without Cup ( $G_\lambda = 0.6$ ,  $f = 405\text{ MHz}$ )

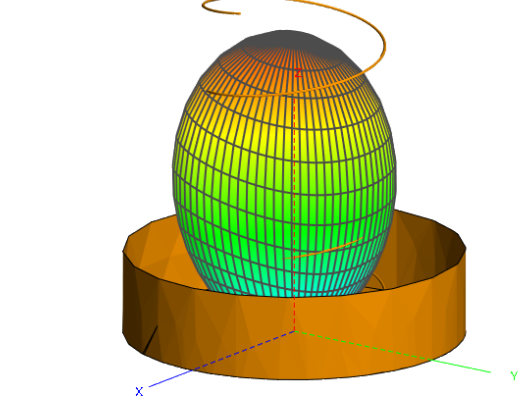


**Figure 4.9:** Simulated Helical Antenna Pattern with Cup ( $G_\lambda = 0.6$ ,  $f = 405\text{ MHz}$ )

It was therefore decided that the antenna would initially be built with a large ground plane and higher number of turns. Then, after measurement results and protocol implementation, the ground plane would be decreased appropriately to fit onto the mount. If time allows, and it is deemed necessary, a cup will then be added to the ground plane, to improve the pattern and antenna performance, and cater for the radiosonde link. The final model parameters are then  $D = 187.1\text{ mm}$ ,  $S = 88.2\text{ mm}$ ,  $n = 4$ , and  $G = 350\text{ mm}$ .

#### 4.5.4 Matching

Impedance matching should be done if the helical antenna is to be fed by a  $50\Omega$  coaxial cable. It was decided to match the antenna to the custom link's frequency of  $f = 433\text{ MHz}$  using the strip method mentioned in Section 2.3.2 for an uncapped ground plane. The FEKO model for this method is shown in Figure 4.10.

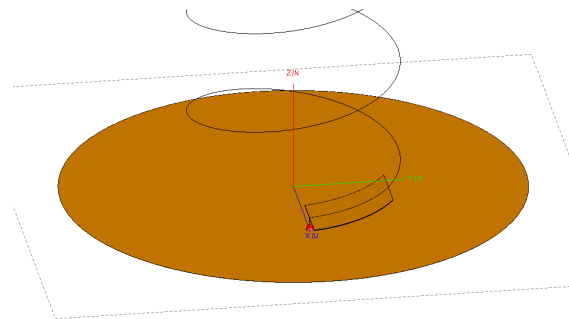


**Figure 4.10:** Helical Antenna with Matching Strip Simulation Model

The strip is recommended to be relatively flat, and extend for approximately the first quarter turn. Its pitch angle was therefore chosen to be half that of the full helix, and it was chosen to extend for 0.15 turns. The unknown parameters for the strip are then its height above the ground plane (also the height of the coaxial pin), and its strip width. The FEKO optimiser was used to optimise these two parameters for a minimum return loss. The resulting return loss as a function of frequency is shown in Figure 4.11. The resultant mismatch loss is close to 0 dB at the target frequency, and 0.451 dB at 405 MHz.

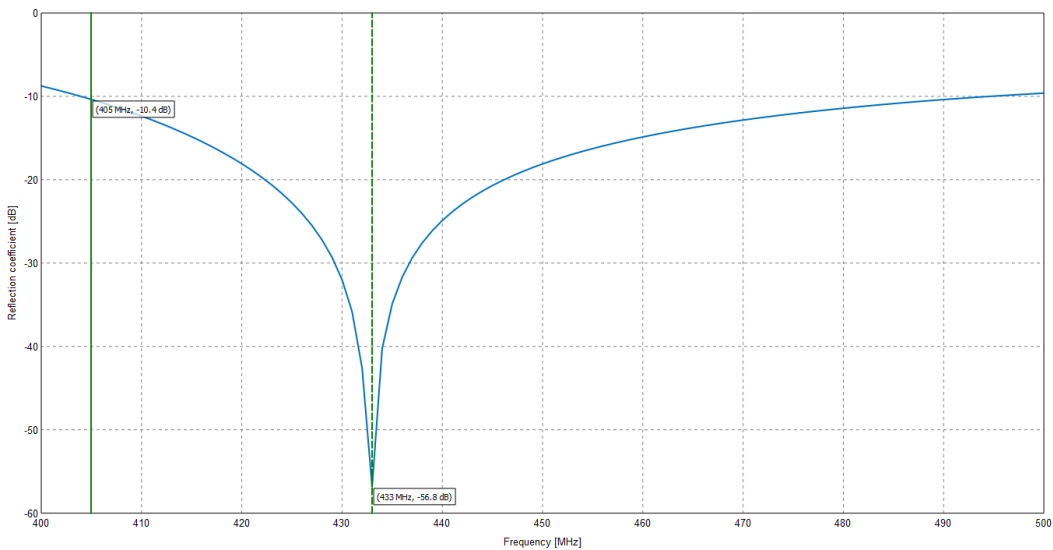


**Figure 4.11:** Simulated Helical Antenna Return Loss vs Frequency

The final antenna parameters are:

Parameter	Value
Diameter (D)	187.1 mm
Turn Spacing (S)	88.2 mm
No. of Turns (n)	4
Ground plane diameter (G)	> 350 mm
Strip height (sh)	19.4 mm
Strip width (sw)	77.7 mm
Strip length (sl)	132 mm
Cup height, if used (ch)	88.2 mm

**Table 4.9:** Helical Antenna Final Parameters

## 4.6 PocketQube Unit Antenna

### 4.6.1 Mechanical Considerations

Since the system is constrained to the 433 MHz band due to the Radiosonde link, the wavelength of interest is relatively large (693 mm). At this wavelength, one half of a half-wavelength dipole is around 173 mm, and the width of a patch antenna on FR4 is around 215 mm. Since the PocketQube is planned to be around 100 mm long, it is clear that a higher frequency band would be more suitable. For the planned prototype balloon satellite launch, it is therefore decided to design a simple half-wavelength dipole, and allow it to protrude out the ends of the PocketQube housing from launch. Recommendations for future projects are given in Section 7.2 (such as using a much smaller but lower efficiency normal-mode helical antenna on the PQ with a higher gain antenna on the GS).

### 4.6.2 Simulation Design and Matching

It was decided to use a simple half-wavelength dipole for the PQ unit, due to its omnidirectional radiation pattern and its extremely easy design and construction. A simple 1.5 mm metal wire will be used due to its availability, with a small gap between the two sides of the dipole, and fed by a coaxial cable.

The design parameters for the dipole are  $L_\lambda$  (the total dipole length relative to lambda),  $F_{\text{gap}}$  (the gap distance of the feed), and  $F_{\text{length}}$ , the length of the feed. A fixed gap distance of  $F_{\text{gap}} = 5$  mm is decided on, as it is assumed to not be critical if sufficiently small.

The FEKO model in Figure 4.12 was used. The optimiser was used to calculate the optimal dipole length and feed length that would minimize the return loss for  $f = 433$  MHz at a feed impedance of  $50 \Omega$ . The resultant parameters are found to be  $L_\lambda = 0.45$  ( $L = 312$  mm)

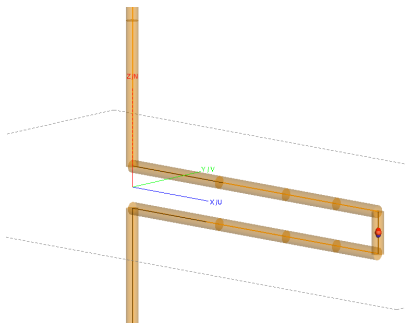


**Figure 4.12:** General Dipole Simulation Model

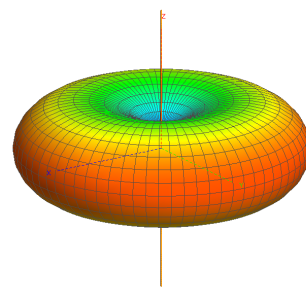


**Figure 4.13:** Simulated  $0.45\lambda$  Dipole Radiation Pattern

and  $F_{\text{length}} = 39.0 \text{ mm}$ . The resultant radiation pattern of the dipole is shown in Figure 4.13, as well as the optimised return loss as a function of frequency in Figure 4.14.

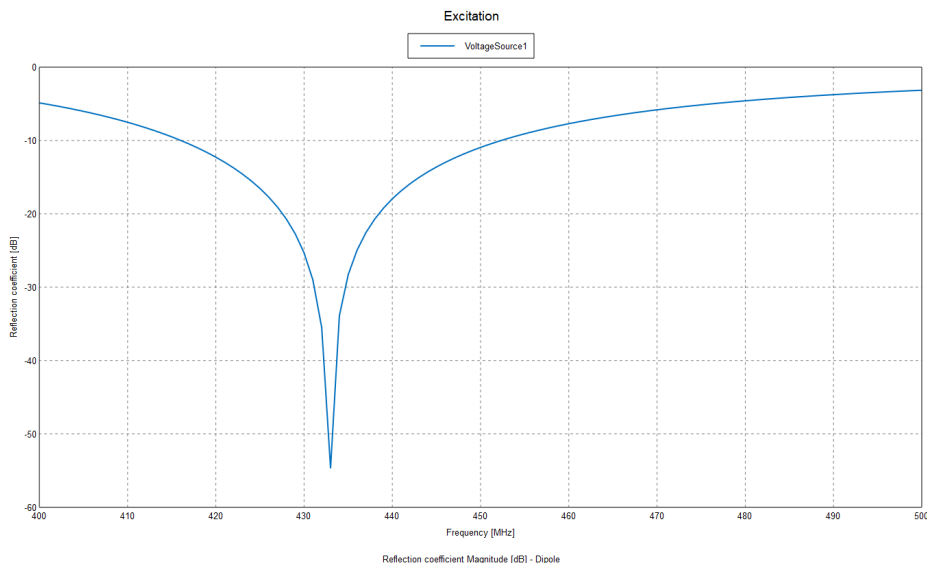


**Figure 4.14:** Simulated  $0.45\lambda$  Dipole Return Loss vs Frequency

## 4.7 Software

### 4.7.1 Classes

The Arduino framework will be used, as well as a custom C++ library for re-usability across GS and PQ code. Tables C.1 to C.6 in the Appendix describe expected class functionality.

Although the CSP protocol was considered, it was decided to rather develop a simple ASCII protocol between the PQ and GS. This flow control is encapsulated in the *link* class. The link object can be set to either *Controller* or *Responder* mode for the GS and PQ respectively, and allows *Telemetry* and *Telecommand* operating modes. In *Telemetry* mode, the responder sends data at regular intervals to the controller, pausing at longer intervals to *listen* for a “telecommand mode” message. If the responder receives this message, it sends an “ACK” message, and switches to *Telecommand* mode to await further commands.

The *PqTnc* and *PqUnit* classes were designed as Singleton classes for the GS and PQ respectively. Here, the GS is referred to as a *Terminal Node Controller* (TNC) with reference to the serial interface it exposes to a host computer. This is summarised in the created *SUNQ* protocol in Appendix B.2.

### 4.7.2 Tracking

For path tracking, it is decided to store data in the TNC object on the ESP32 itself, instead of streaming it from the host computer. This is so that the host can be disconnected, and the payload will still be tracked.

An "instant" is defined as both a location and a time. The *PqTnc* object performs a check in its update loop to determine if an instant has been reached, based on its GPS received time. The *GroundStation* object should store two locations - the previous location in the path, and the location it is moving towards. The mount is pointed at the location which linearly interpolates between these two instants, with a factor based on the current time, and the time of the two instants.

To allow direct GPS tracking and flight path tracking to be used simultaneously, it was decided to follow the flight path data until a location from the satellite is received. When a "known" location is received, it is used for a specified timeout "trust" period, until a new location is received and is overwritten. A pseudo low-pass filter is added to the ground station to prevent pointing "jitter". The final algorithm is shown in Figure 4.15.

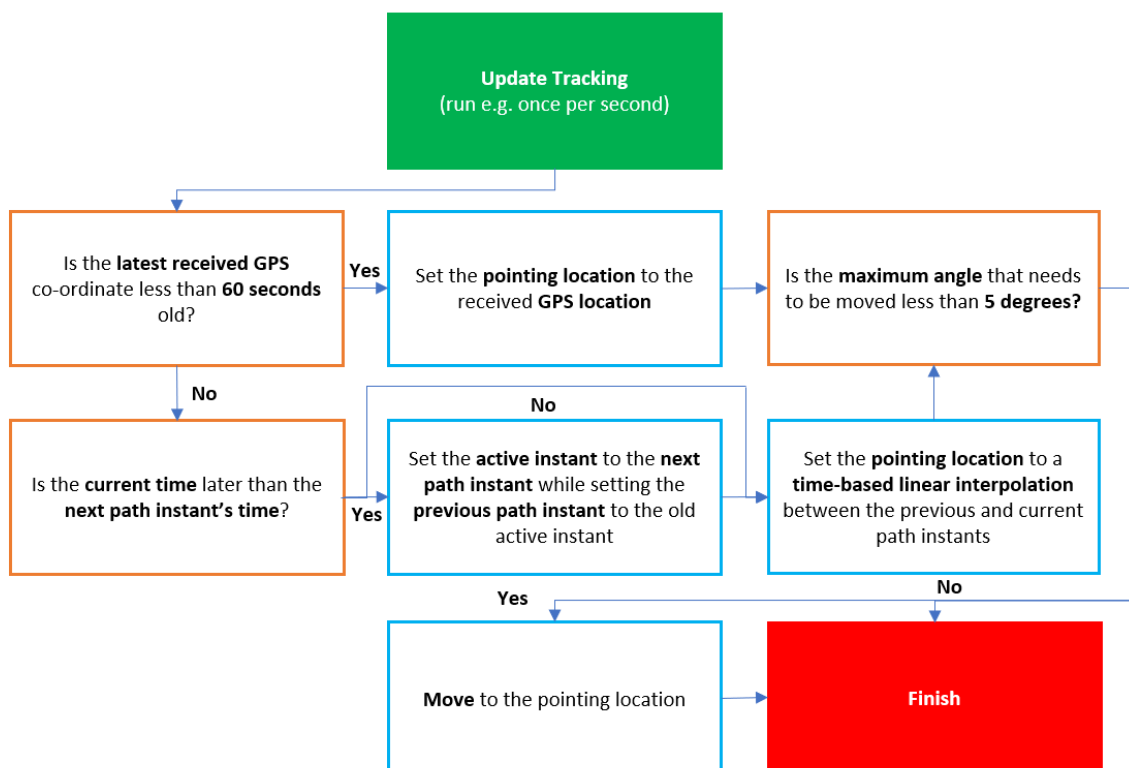


**Figure 4.15:** Tracking Algorithm Flow Diagram

# 5. Implementation

## 5.1 Ground Station PCB

The ground station PCB was manufactured in-house. A figure of the PCB with components assembled, as well as a helical antenna attached for initial development, and a simple monopole GPS antenna, is shown in Figure 5.1. Due to a few incorrect layouts on the PCB, some additional wired connections were made. A list of errata can be found in Appendix C.4.

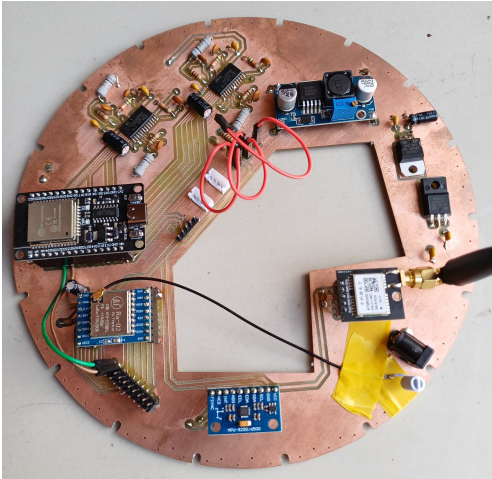


**Figure 5.1:** Ground Station PCB Implementation



**Figure 5.2:** Ground Station Initial Antenna Implementation

## 5.2 Ground Station Antenna

The initial helical antenna build is shown in Figure 5.2. 2.5 mm stranded copper wire was used due to its flexibility and availability. A cardboard ground plane wrapped in aluminium foil was used due to its lightweight nature. Further, a strip of harder aluminium tin was taped to the wire for the matching strip. Initially, the strip was over-sized, and more turns than necessary were used. A female panel-mounted SMA connector was mounted using bolts, and the antenna wire was soldered to the protruding pin.

The coiled wire is mechanically supported by a central PVC pipe and wooden dowels. Markings on the pipe were used to dimension the antenna. The materials were sized to provide stability, but not exceed the maximum torque limitations of the motors. The

final antenna weight was measured at 344 g, giving a worst-case mass-distance product of  $344 \text{ g} \times \frac{45 \text{ cm}}{2} \approx 0.08 \text{ kg} \cdot \text{m}$ , which is under the maximum of 0.2 kg · m.

After initial testing, the matching strip was cut to size, a circular trapezoidal cut-out was made to support a lower elevation angle, and the number of turns was set to  $n = 4$ . The system was eventually mounted onto a tripod, and a final photo of the full ground station out in the field is shown in Figure 5.3.



**Figure 5.3:** Ground Station Mounted on Tripod

### 5.3 PocketQube Unit PCB

Unfortunately, not enough prototypes were ready for an end-project University balloon launch. The power for the PQ unit was therefore implemented using large but readily available converters/regulators. In a final launch, however, this power section would either be replaced by the EPS, or a single, very low drop-out voltage regulator to convert the LiPo 3.7 V to a useable 3.3 V.

The PQ unit PCB was ordered through an external supplier (JLCPCB). In order to begin initial development and testing, a breadboard prototype was initially created using an Arduino Nano, as shown in Appendix D.2. Since the Nano has the same MCU as the designed PCB, the developed software could then simply be flashed onto the PQ unit using an off-board programmer.

The final module is shown in Figures 5.4 and 5.5. As noted in the errata in Appendix C.4, the crystal's loading capacitors were mistakenly left out. The MCU's internal 8 MHz clock was therefore used. This clock, however, is generally badly calibrated, and resulted in software serial communication with the GPS module initially not working. This was fixed by setting the OSCCAL register in software to calibrate the clock.

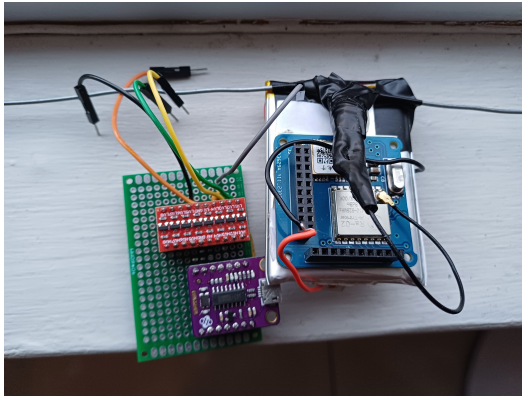


**Figure 5.4:** PQ Unit (front) [right] and programmer [left]

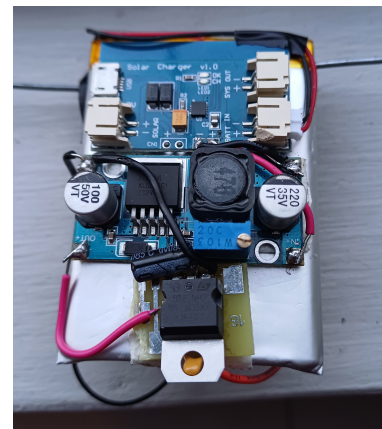


**Figure 5.5:** PQ Unit (back)

The board was first bootloaded with an Arduino Nano, and then the programmer circuit in Figure 5.4 was developed to flash the board via UART. The programmer consists of a CH340 USB-to-serial module, a reset RC filter, as well as a 3.3V to 5V level converter (since the PocketQube PCB is designed to run at 3.3V). The board and dipole antenna was mounted onto the 2000 mAh LiPo battery. The power section consists of a LiPo charger, a boost converter module, and a 3.3V linear voltage regulator circuit.

## 5.4 PocketQube Unit Antenna

The PQ unit antenna was simply implemented using readily available 1.5 mm steel wire. The wire was bent manually and the end of u.FL pigtail cable was stripped and soldered to the wire. Lastly, insulation tape was added near the connection for stability and protection. The final design can be found in Appendix D.2.

## 5.5 Software

The following documents notable choices made during implementation, but after design. All code is available at <https://github.com/gvcallen/pqcom/tree/main/code>.

### 5.5.1 Mount Control

The motors were setup in half-stepping mode at maximum current. The step sequence (as in the driver datasheet [31]) was implemented using an array. The two-axis mount requires some relatively involved control. Elevational variation is straight-forward, as the azimuthal motor (controlled by Gear C in Figure 3.4) can be held fixed, and the elevation motor (Gear D) stepped accordingly. For azimuthal variation, if the elevation motor is held fixed, rotating the azimuthal motor causes the mount to also change in elevation, which must be compensated (demonstrated in Appendix D.3). The “azel” ratio is the number of elevation motor turns required to tilt the elevation axis the same amount as the azimuthal motor, given by:

$$\text{azelRatio} = \frac{D_{\text{outer}}/B}{C/A} = \frac{92/20}{60/15} = 1.15 \quad (5.1)$$

The azimuthal and elevation angles can then be calculated as in Formulae 5.2 and 5.3, where *elRev* and *azRev* are the number of elevation/azimuth motor steps per full revolution (equal to  $200 \times \frac{92}{20} \times \frac{140}{80} = 1610$  and  $200 \times \frac{60}{15} = 800$  respectively).

$$\text{azAngle} = \text{azPos} \times \frac{360^\circ}{\text{azRev}} \quad (5.2)$$

$$\text{elAngle} = (\text{azPos} \times \text{azelRatio} + \text{elPos}) \times \frac{360^\circ}{\text{elRev}} \quad (5.3)$$

The number of simultaneous "delta" steps to make in order for each axis to move to a new location  $\{\text{newAzAng}, \text{newElAng}\}$  implemented in *setAzimuthElevation()* is then given by Formulae 5.4 and 5.5. Then, to smoothly step both motors simultaneously, speeds are set according to the ratio *deltaAzSteps* : *deltaELSteps*. A conversion from cartesian to azimuthal-elevation is then done to allow a boresight vector as input.

$$\text{deltaAzSteps} = \text{angToPosAz}(\text{newAzAng}) - \text{azPos} \quad (5.4)$$

$$\text{deltaElSteps} = -\text{deltaAzSteps} \times \text{azelRatio} + \text{angToPosDeltaEl}(\text{newElAng} - \text{elAng}) \quad (5.5)$$

### 5.5.2 Pointing

A small C++ header-only library titled *wgs84* was used to perform a Mercator projection to cartesian co-ordinates, with Cape Town as the origin. This allows a pointing vector to be determined, which could be passed to the mount and set as the boresight. Unfortunately, the purchased IMU (the MPU-9250) was found to be counterfeit and did not include a magnetometer. A constraint was therefore made that the ground station should be manually faced towards magnetic north using a compass, and then angle between the zero sensor and magnetic north was manually measured as a reference input.

### 5.5.3 Radio and GPS

Existing Arduino libraries were wrapped into "cover classes", with the library *Radiolib* initially being used for communication with the LoRa module. However, it was found that its implementation was too large in program size for the Atmega328. It was therefore replaced with a smaller implementation, *LoRaLib*. For the GPS, *TinyGPSPlus* was used.

### 5.5.4 GUI

A simple GUI application was developed using the Qt framework to ease testing and flight path uploading. The ability to import a CSV in the format provided by *HabHub* was provided. An image of this application can be found in Appendix E.1.

# 6. Testing

## 6.1 Ground Station PCB

After implementation, trivial initial tests were done to ensure the ground station was functional. This included ensuring all modules (radio, GPS and IMU) could be interfaced with successfully, as well as a few more detailed power tests, documented below.

### 6.1.1 Power

During no load from the motors, but load from the integrated circuits, the voltage readings in Table 6.1 were obtained. The GPS and ESP lights were noted to be on. From these tests, it is clear that the full power system is working as expected.

Component	Expected	Measured
LD1117	3.3 V	3.307 V
LM7805	5 V	5.069 V
XL6009	24 V	24.07 V

**Table 6.1:** Ground Station Voltage Measurements

The current consumption through a 12.3 V supply was measured at 179 mA with all systems on except the motor drive. This equates to around 2.2 W of power. Since a total of around 1 W of power is expected during no transmission as calculated previously, this means that the voltage regulators are dissipating the remaining 1.2 W. This is well within the limitations of both regulators e.g. the LD1117 can dissipate a theoretical maximum of 12 W. The system was left idle for an hour with no noticeable change in current or heat.

### 6.1.2 Motor Drive

The motor drive system was tested with the half-step sequence implemented as previously mentioned. Current measurements were made for different operating conditions and are listed in Table 6.2. Tests 1-4 were conducted using a *calibrate - return to stow* cycle repeated 10 times at 2/3 maximum current. The intentions of these tests was to determine the speed limitations of the system, since it is easy to identify if the system misses steps by moving it back and forth continuously. Tests 5-6 were conducted with the mount stationary at around

75 degrees elevation at 2/3 and 3/3 current respectively. These tests were intended to stress test the current handling and heat dissipation capabilities of the system. Note that the idle current of 179 mA was subtracted from each measurement.

Test No.	Description	$I_{\min}$ (A)	$I_{\max}$ (A)	Observation
1	40 ms step delay			No noticeable steps missed
2	20 ms step delay	0.669	0.961	No noticeable steps missed
3	10 ms step delay	0.559	-	Small slip near calibration start
4	5 ms step delay	0.252	-	Large number of steps missed
5	2/3 current; 1 hour	0.712	0.713	Minimal system change across the hour
6	3/3 current; 1 hour	2.031	2.261	Stabilised current but very hot mount

**Table 6.2:** Motor Drive Operating Tests @ 12 V supply

Since the boost converter operates as a DC transformer, the current consumed by the motor drive near the start of the hour can be calculated as  $2.031 \times \frac{12}{24} \div 2 = 0.509$  A. This is slightly higher than the designed reference current of 475 mA, however it is assumed that the L6219 was dissipating the remainder, since it was observed to increase in temperature. Since the system is stable near the end of the hour, and the L6219 has thermal shutdown, the system is considered to be within a safe operating region, even though it is clear the power dissipated in the driver increased throughout the hour.

## 6.2 PocketQube Unit PCB

As mentioned, it was decided that a balloon satellite would not be flown by the department. Therefore, integration with the other PocketQube modules was not prioritised for the PCB and the RS-485 line drivers were left off the board. Current consumption for the rest of the components, however, was measured at 31 mA when the system was directly powered from a power supply running at 3.3 V. This is only 6 mA lower than the total current expected from the GPS and MCU ICs, indicating conformance to the original design.

## 6.3 Ground Station Antenna

The ground station antenna's return loss was measured using a network analyser to ensure it was correctly matched to  $50\Omega$ . The resultant graph is shown in Figure 6.1. The figure shows the simple matching strip design is effective and was implemented correctly, however it should be noted that the null is not as deep as simulated (only around -10 dB minimum at 427 MHz as opposed to the -50 dB simulated minimum at the centre frequency of 433 MHz).

There are several reasons why the null may not be as deep as simulated. Firstly, the aluminium foil used is far from an ideal PEC. Secondly, the imperfections in the antenna's construction (e.g. bends in the coil wire, the PVC and wooden dielectrics that were not

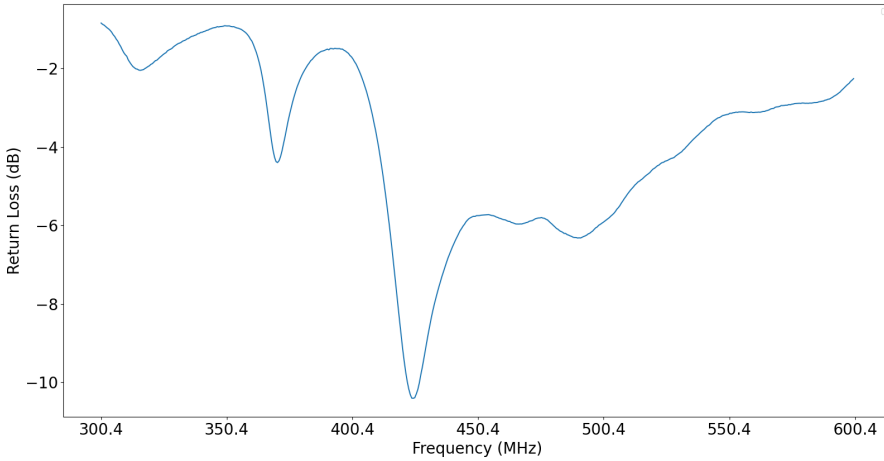


**Figure 6.1:** Measured Helical Antenna Return Loss vs Frequency

simulated, etc.) may cause the match to be non-ideal. Finally, it is hypothesized that a longer strip might have made the implementation more practically realizable, due to the increased capacitive coupling and decreased fringing effects which the matching technique relies on. Instead of optimizing the antenna build, however, it was decided to run further tests with this system, since the link budget allows for up to a 1 dB matching loss. optimisation is therefore left for future projects. Lastly, the antenna gain pattern unfortunately could not be measured, as a chamber was not available that catered for the low frequency of the system.

## 6.4 PocketQube Unit Antenna

The return loss of the PQ dipole antenna is shown in Figure 6.2. It is clear that, due to the antenna's simple construction, the resulting match is near-perfect. Since frequencies from around 420 to 440 MHz provide less than 0.1 dB mismatch loss, the final system frequency will be determined by the helical antenna only.

## 6.5 RF Module

### 6.5.1 Setup

The radio module and communication link were initially tested/characterised using two small, off-the-shelf helical antennas, before integrating the custom-built antennas. The helical antennas managed an initial range of around 50 m in an urban area with a LoRa spreading factor of 8. This was tested with the one antenna near a window indoors, and the second antenna inside a car. This test served merely as a "proof-of-concept", and was not intended as an indication of system performance.

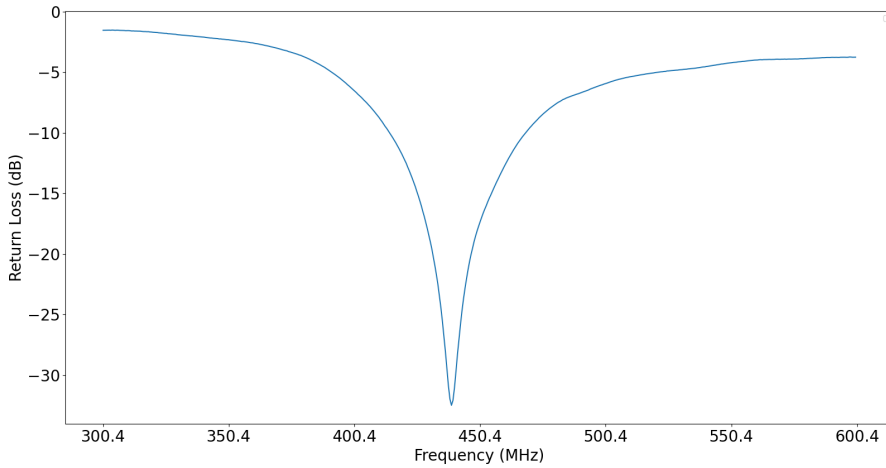


**Figure 6.2:** Measured Dipole Antenna Return Loss vs Frequency

### 6.5.2 Transmit Power Consumption

The custom-built antennas were then connected to both the PQ and the GS and more detailed tests were conducted. The first test measured the power consumption for the PQ unit as a function of transmit power. This is displayed in Figure 6.3, after subtracting a 31 mA "no-transmit" current. The maximum current is around 96 mA for the maximum output power (quoted by the RA-02 as 18 dBm +/- 1 dBm).

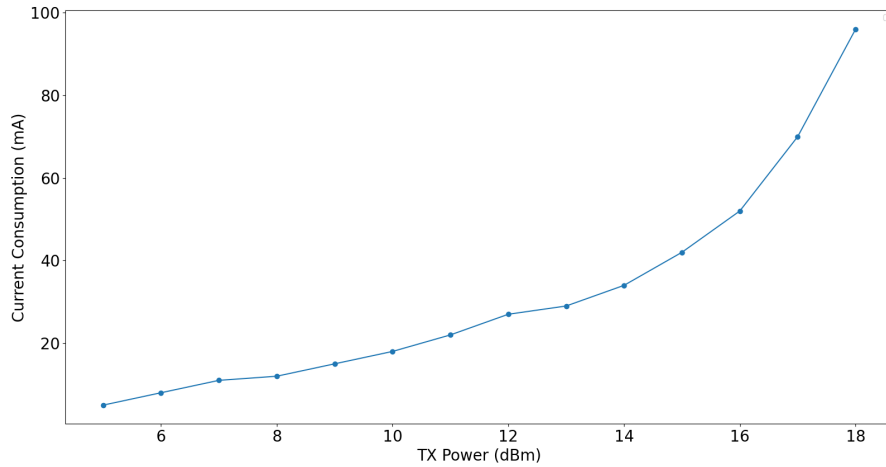


**Figure 6.3:** TX Output Power vs Current Consumption

### 6.5.3 Data Rate

To test the possible bit rates as a function of LoRa spreading factor (SF), two RA-02 modules were setup with the same parameters and the bit rate was measured as the SF value was varied. A payload length of 255 was used, with 4/6 CRC, an 8 bit preamble, 500 kHz bandwidth,

and a 10 ms delay between packets. The bit rate was then measured on the receiving side and is shown in Table 6.3.

Spreading Factor	Theoretical Bit Rate (bps)	Measured Bit Rate (bps)
7	18229	17200
8	10417	10240
9	5859	5800
10	3255	3320
11	1790	1846

**Table 6.3:** LoRa Bit Rate vs Spreading Factor

The results show that the system is set up correctly, and that a spreading factor of 8 is the correct choice to achieve the 9600 baud rate requirement.

## 6.6 Serial Protocol

Basic serial protocol tests still to be added if necessary, however the serial commands are currently working properly

## 6.7 Range

Line-of-sight range tests were conducted. Both antennas were manually positioned to determine the system's capabilities. Various measurements were done at the originally designed parameters (e.g. SF 8, CR 4/6, 500 kHz) and with automatic gain control (AGC). The resulting *received signal strength indicator* (RSSI), signal-to-noise (SNR) ratio, and packet reception rate (PRR i.e. percentage of non-corrupted packets received) was recorded. For the unfamiliar reader, the highest (best) theoretical RSSI is 0 dB, and the minimum SNR for SF 8 is -10 dB (LoRa is capable of demodulating negative signal-to-noise ratios).

Test No.	Range	GS Location	PQ Location	Comments
1	1.4 km	Firgrove Way	M3 Bridge	
2	4.6 km	Constantia	Silvermine	Cloudy conditions
3	9.7 km	Boys' Drive	Simon's Town	
4	34.5 km	Steenbras	Simon's Town	
5	49 km	Takara Stellenbosch	Silvermine	Optimal transmitter placement uncertainty

**Table 6.4:** Range Test Locations

Tests were done in locations around the Western Cape. These locations are described in Table 6.4 and mapped out in Appendix F.1. The first primitive test (which is not listed) was a 300 m test on Coetzenburg field in Stellenbosch. The performance of this test was

found to be low compared to subsequent tests, with an RSSI of around -92 dBm recorded. It is assumed that ground bounce was the major contributing factor to this, due to the low operating frequency of the system (around 430 MHz) and the close proximity (around 1m) the antennas had to the ground.

The final results are plotted as a function of distance in Figures 6.4 and 6.5, with a logarithmic curve fit. All measurements were taken as an average of at least 10 consecutive samples. The dipole was both horizontally and vertically placed. The packet contents were verified using a packet ID, the GPS location of the transmitter, as well as inspecting whether a CRC (Cyclic Redundancy Check) error had occurred. If any of these were incorrect, the packet was considered "missed".

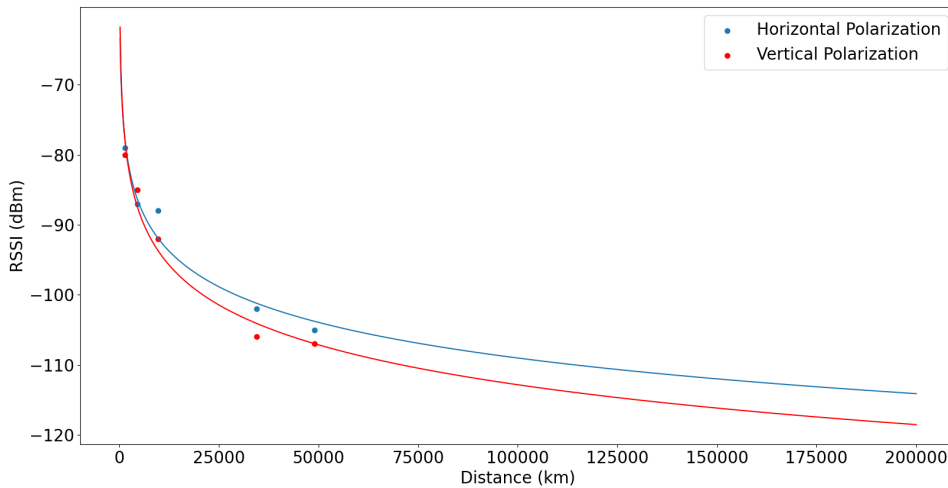


**Figure 6.4:** Measured RSSI vs Distance

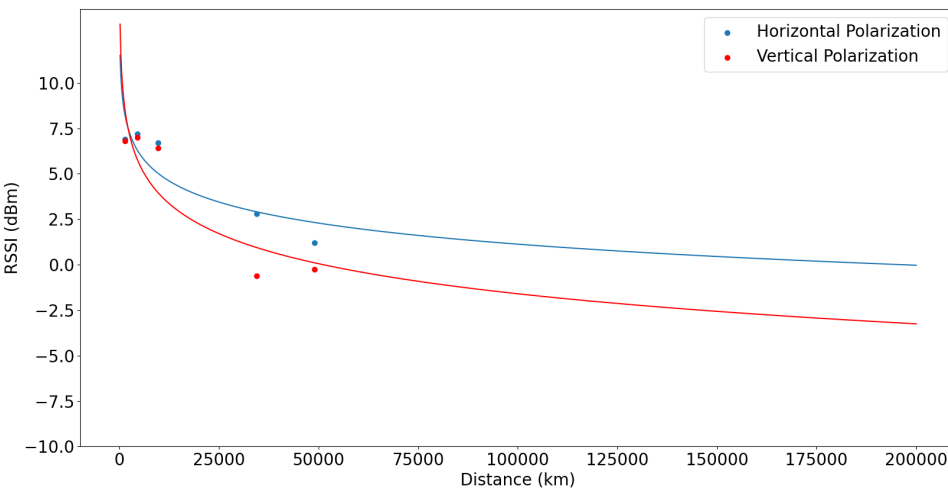


**Figure 6.5:** Measured SNR vs Distance

The data shows that the system would successfully meet the 110 km range requirement. No CRC errors were found once the system was in steady state for all tests. The final test at

50 km recorded an RSSI of around -107 dBm for the vertically polarized case. The predicted RSSI for vertical polarization at 125 km is around -114 dBm, whereas the receiver sensitivity is as low as -119 dBm, indicating a 5 dB margin. It should be noted that the SNR logarithmic fit is not considered reliable, since the receiver appears to adjust the gain to keep the SNR around 7.5 dB for closer distances. However, the RSSI appears to follow a logarithmic curve as predicted by the free space path loss formulae.

## 6.8 Tracking and Pointing

### 6.8.1 Open-Loop

In order to test the GPS pointing and open-loop tracking, a map was printed with lines pointing to nearby locations, from a pre-determined location as the origin. The ground station was then placed on top of this map at this location, and positioned to face magnetic north using a compass. This test had multiple goals i.e. to simultaneously test the mount transfer function, the GPS co-ordinate pointing, and the flight path data tracking. An image of the test setup is shown in Figure 6.6.



**Figure 6.6:** Pointing Test Setup

Flight path data containing the pre-determined co-ordinates was uploaded to the system, and the azimuthal angle was qualitatively confirmed to point in the directions labelled on the map using a ruler. Further, the elevation angle was measured using a protractor and compared against the expected angle. The system was found to successfully point towards the commanded locations at the desired times. The measured elevation angle was found to be within 5° of the expected angle. This is considered to be within the limitations of the

measurement system (the setup to measure the incline angle of the ground plane was non-ideal due to the bends in the ground plane and the awkward measurement procedure). Ideally, an accurate inclinometer should be used to confirm the elevation angles.

### 6.8.2 Closed-Loop

The closed-loop received location GPS tracking was tested on an open field with close to 300 m range. The PQ unit was carried around the field transmitting its GPS location, and the RSSI, as well as the antenna pointing direction, were recorded/observed.

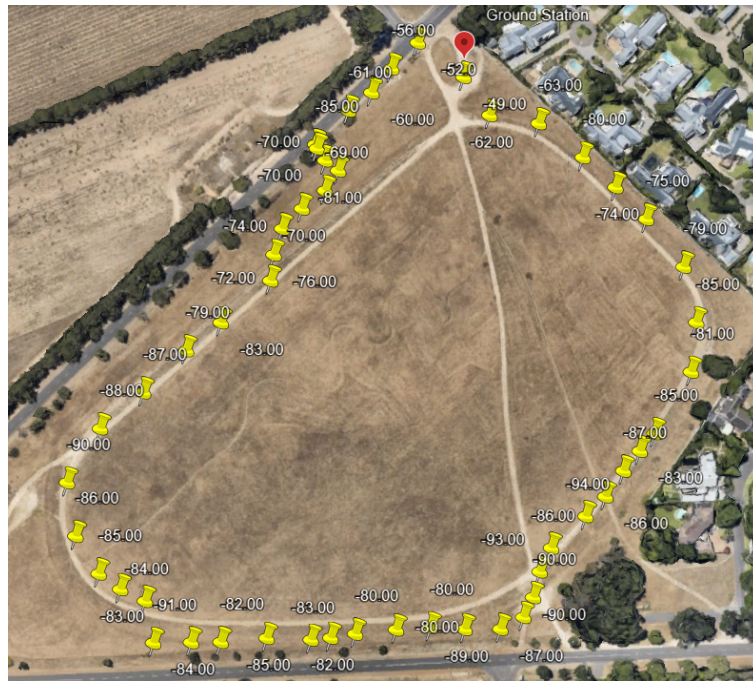


**Figure 6.7:** GPS Tracking Locations and RSSI Values

The system was observed to successfully track the transmitter around the entire field without noticeable delay, until it reached a distance of around 10 m, where the pointing direction became unpredictable. This is attributed to the low accuracy of the GPS modules. Since the system is already known to have the capabilities of pointing at a GPS location (from the open-loop tests) and the time requirement is much lower for the balloon satellite system (which requires a tracking speed on the order of 45 degrees in an hour or two) it can be said that the system works as designed.

The above test also serves as a primitive test for GPS accuracy. The width of the main path being walked on was 3.2 m wide. The furthest mapped deviation of a received GPS co-ordinate from this path is measured at around 3 m (note that the map image is outdated). An upper bound on the GPS's accuracy can be therefore be said to be 6.2 m. It is clear that this far exceeds the system requirements laid out in Section 4.1.1.

## 6.9 Radiosonde

The helical antenna was setup to receive the radiosonde GFSK signal using the RTL-SDR USB dongle and an SMA to MCX adapter. A resultant "squench" signal was observed to be received in one second intervals, and the frequency domain of this signal is plotted in Figure 6.8 using GNU Radio software. A free Python script *Auto-RX* was found to cater for receiving telemetry from the iMet-54 Radiosonde, and the GPS location was successfully received. The developed GUI was therefore altered to allow for tracking the external Radiosondes, and the closed-loop tracking was successfully tested with a similiar but shorter-range procedure as in 6.8.2.

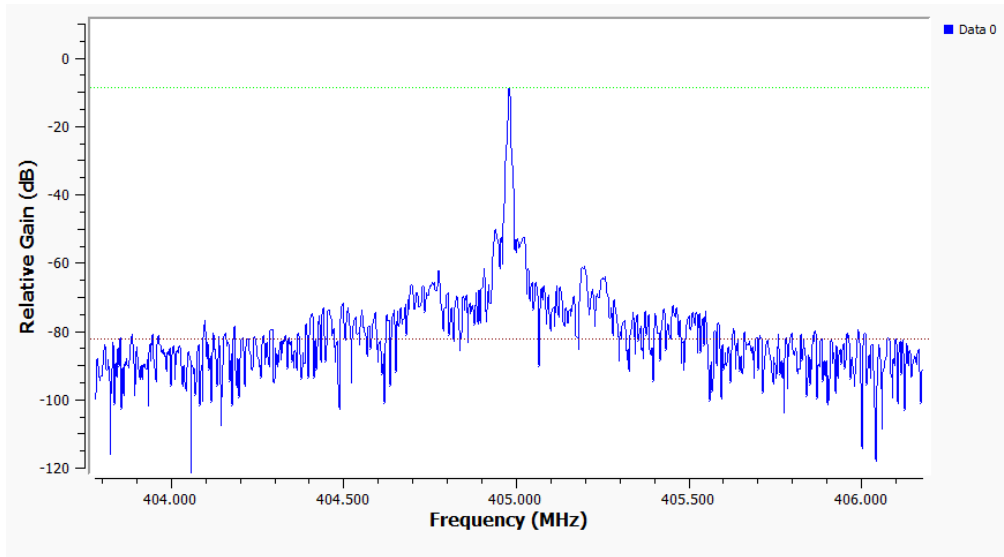


**Figure 6.8:** Received Radiosonde Signal FFT

## 6.10 Full System

The South African Weather Service fortunately granted permission for tracking of their weather balloons, which contain similar Radiosondes as designed for. A full system test was therefore conducted, with closed-loop tracking being prioritised. The system was found to successfully track and receive the Radiosonde's GPS location up to a distance of 50 km. It should be noted that, since the Radiosonde's receiver has a low sensitivity, a range as long as the custom link is not expected. However, this full system test successfully demonstrates the capabilities of the system. An image of the setup is shown in Figure xxx.

# 7. Conclusion

## 7.1 Summary

A PocketQube communication system, with a tracking ground station and a PocketQube PCB module, was successfully designed to meet the system requirements for a balloon satellite launch in Saldanha Bay. Unfortunately, the launch did not take place, however several modularized tests helped to prove that the system is fully functional and capable of communicating over the required distances.

LoRa proved to be a viable choice for the communication link. Not only did the link meet the throughput requirements, but the increased immunity due to the spread-spectrum technology suggests that it should be made a priority choice for satellite communication links, given that the required bandwidth is available. The helical antenna design also proved to be effective in the context of the project, as it was easy to manufacture and provided high gain and bandwidth for relatively low effort compared to alternatives.

The open-loop tracking method was successfully implemented, however would need to be tested in a full system test to confirm its accuracy. Closed-loop GPS tracking was shown to work over a short-range, and is likely the preferred tracking method, given that an initial communication link can be established with the satellite. Lastly, the final ground station and PocketQube module PCB designs and implementations were shown to be effective, and provide a good foundation for future work.

## 7.2 Future Work

There are various improvements and alternative choices that can be explored in the context of the developed system:

- *Improved ground station PCB.* The ground station PCB was designed to use break-out boards, through-hole components, and modules for rapid development. Future designs could replace almost all components with surface-mounted ones, and remove break-out boards (e.g. the ESP32 board) to reduce cost, improve connection integrity, and allow more space for additional components.
- *Improved helical antenna construction.* The ground station antenna can be optimised,

by constructing it using more rigid materials, as well as stricter manufacturing procedures. This would hopefully decrease the variance between the simulation and the implementation, and improve the matching and radiation pattern. A longer antenna with higher gain could also potentially be implemented if similar materials are used, considering that the mass-distance product of the implemented antenna was under half of the theoretical maximum.

- *PocketQube antenna integration.* The antenna for the PocketQube was not designed to be deployable, but the half-dipole was shown to provide an effective proof-of-concept. For integration into future PocketQubes, options include using a higher frequency band; making the antenna foldable with a spring mechanism; or using a much lower efficiency normal-mode helical antenna.
- *Radiosonde link optimisation.* The radiosonde link and integration was not fully explored. For example, a dedicated, more sensitive transceiver targeted at the relevant frequency (as opposed to a generic software-defined radio) could be explored. This might require an RF switch, which would provide the ability to change between the custom and radiosonde link in software.
- *Signal strength scanning.* Faster signal strength "conical" scanning could be explored. Although it was not investigated in this project (as a brute-force scan or open-loop estimate is generally sufficient to initially find the payload and receive its GPS location) the flexibility of tracking the payload using only its received radio signal may be beneficial.

# Bibliography

- [1] rose.edu, “Rsc cyber students fly high with high altitude balloon launch,” <https://www.rose.edu/content/news-events/news/2018/06-june/rsc-cyber-students-fly-high-with-high-altitude-balloon-launch/>, [Accessed 25-10-2023].
- [2] D. Slabber, “Pocketcube mechanical interface,” [Accessed 16-08-2023].
- [3] “Tracking a Weather Balloon; High Altitude Science,” <https://www.highaltitudescience.com/pages/tracking-a-weather-balloon>, [Accessed 13-08-2023].
- [4] C. R. A. Inc, “How to make a 433 mhz yagi antenna design for a long-range?” <https://lcantennas.com/433-mhz-yagi-antenna-design-for-a-long-range/>, 2022, [Accessed 16-08-2023].
- [5] Wikipedia, “Inverted-f antenna,” [https://en.wikipedia.org/wiki/Inverted-F\\_antenna](https://en.wikipedia.org/wiki/Inverted-F_antenna), 2023, [Accessed 16-08-2023].
- [6] Celestis, “What are the ”azimuth” and ”elevation” of a satellite?” <https://www.celestis.com/resources/faq/what-are-the-azimuth-and-elevation-of-a-satellite/>, [Accessed 29-09-2023].
- [7] A. Wonggeeratikun, S. Noppanakeepong, N. Leelaruji, N. Hemmakorn, and Y. Moriya, *The Analysis of the Airplane Flutter on Low Band Television Broadcasting Signal*. ResearchGate, 2023.
- [8] P. J. Bevelacqua, “Antenna theory,” <https://www.antenna-theory.com/>, 2022, [Accessed 16-08-2023].
- [9] “Weather Balloons — weather.gov,” [https://www.weather.gov/bmx/kidscorner\\_weatherballoons](https://www.weather.gov/bmx/kidscorner_weatherballoons), [Accessed 12-08-2023].
- [10] Sondehub, “Hab-hub flight path predictor,” <https://predict.habhub.org/>, [Accessed 15-07-2023].
- [11] Ringbell, “Distance to the horizon calculator,” <http://www.ringbell.co.uk/info/hdist.htm>, [Accessed 15-07-2023].

- [12] Omni-Calculator, “Radar horizon calculator,” <https://www.omnicalculator.com/physics/radar-horizon>, [Accessed 15-07-2023].
- [13] Intermet, “imet-54,” <https://intermet.co/wp-content/uploads/iMet-54-403MHz-GPS-Radiosonde-Brochure-V5.5.pdf>, [Accessed 13-08-2023].
- [14] “A multi frequency deployable antenna system for delfi-pq,” [https://pure.tudelft.nl/ws/portalfiles/portal/57402203/2019\\_f\\_74.pdf](https://pure.tudelft.nl/ws/portalfiles/portal/57402203/2019_f_74.pdf), [Accessed 13-08-2023].
- [15] R. Israel, “Mercator’s projection,” <https://personal.math.ubc.ca/~israel/m103/mercator/mercator.html>, [Accessed 29-09-2023].
- [16] “Prediction and Tracking a Balloon — Stratospheric Ballooning Association — strato-balloon.org,” <https://www.stratoballoon.org/tracking>, [Accessed 13-08-2023].
- [17] C. A. Balanis, “Antenna theory analysis and design,” [Accessed 29-09-2023].
- [18] sgcderek, “Helical antenna calculator,” <https://sgcderek.github.io/tools/helix-calc.html/>, [Accessed 29-09-2023].
- [19] “A compact low-profile ring antenna with dual circular polarization and unidirectional radiation for use in rfid readers,” <https://ieeexplore.ieee.org/stamp/stamp.jsp?arnumber=8822972>, [Accessed 03-09-2023].
- [20] LinkedIn, “What are the benefits and drawbacks of using different modulation and coding schemes for satcom?” [https://www.linkedin.com/advice/0/what-benefits-drawbacks-using-different-6f#:~:text=The%20most%20common%20digital%20modulation,quadrature%20amplitude%20modulation%20\(QAM\).](https://www.linkedin.com/advice/0/what-benefits-drawbacks-using-different-6f#:~:text=The%20most%20common%20digital%20modulation,quadrature%20amplitude%20modulation%20(QAM).), [Accessed 29-09-2023].
- [21] —, “What are the benefits and drawbacks of using different modulation and coding schemes for satcom?” <https://www.linkedin.com/advice/0/what-advantages-disadvantages-using-qam-over>, [Accessed 29-09-2023].
- [22] Semtech, “137 mhz to 1020 mhz low power long range transceiver,” <https://www.semtech.com/products/wireless-rf/lora-connect/sx1278>, [Accessed 23-10-2023].
- [23] J. Fernandez, “Link budget calculation,” <https://github.com/FOSSASystems/FOSSASAT-1/blob/master/FOSSA%20Documents/FOSSASAT-1%20Link%20Budget.pdf>, [Accessed 29-09-2023].
- [24] M. Arias, “Small satellite link budget calculation,” [https://www.itu.int/en/ITU-R/space/workshops/2016-small-sat/Documents/Link\\_budget\\_uvigo.pdf](https://www.itu.int/en/ITU-R/space/workshops/2016-small-sat/Documents/Link_budget_uvigo.pdf), [Accessed 05-10-2023].
- [25] K. Cheung, “The role of margin in link design and optimisation,” [https://s3vi.ndc.nasa.gov/ssri-kb/static/resources/15-0025\\_A1b.pdf](https://s3vi.ndc.nasa.gov/ssri-kb/static/resources/15-0025_A1b.pdf), [Accessed 23-10-2023].

- [26] I. Campbell Scientific, “The link budget and fade margin,” <https://s.campbellsci.com/documents/us/technical-papers/link-budget.pdf>, [Accessed 05-10-2023].
- [27] GOMspace, “Cubesat space protocol (csp),” [Accessed 24-10-2023].
- [28] E. E. Harstad, “Analysis of balloon trajectory prediction methods,” <https://www.iastatedigitalpress.com/ahac/article/8334/galley/7926/view/>, [Accessed 10-10-2023].
- [29] L. Engineering, “High torque motor,” <https://cnctar.hobbycnc.hu/ZOTYK%C3%93/NEMA%2017%20motorom%20adatlapja%204218M-01.pdf>, [Accessed 13-08-2023].
- [30] Fairchild, “Slotted optical switch,” <https://media.digikey.com/pdf/Data%20Sheets/Fairchild%20PDFs/H22A1,2,3.pdf>, [Accessed 29-09-2023].
- [31] STMicroelectronics, “L6219 stepper motor driver,” <https://www.mantech.co.za/datasheets/products/L6219.pdf>, [Accessed 29-09-2023].
- [32] Gravitech, “Arduino nano,” <https://www.arduino.cc/en/uploads/Main/Arduino-Nano-Rev3.2-SCH.pdf>, [Accessed 29-09-2023].
- [33] J. D. Kraus, “Antennas for all applications,” [Accessed 29-09-2023].
- [34] Intermet, “imet-3100m,” <https://intermet.co/wp-content/uploads/iMet-3100M-403MHz-Military-Antenna-Receiver-Brochure-V4.5.pdf>, [Accessed 12-08-2023].
- [35] A. Devices, “Max2659 gps/gnss low-noise amplifier,” <https://www.analog.com/media/en/technical-documentation/data-sheets/MAX2659.pdf>, [Accessed 18-08-2023].
- [36] u blox, “Neo-6,” [https://content.u-blox.com/sites/default/files/products/documents/NEO-6\\_DataSheet\\_%28GPS.G6-HW-09005%29.pdf](https://content.u-blox.com/sites/default/files/products/documents/NEO-6_DataSheet_%28GPS.G6-HW-09005%29.pdf), [Accessed 18-08-2023].
- [37] “Review of tracking methods,” <http://www.jstor.com/stable/73457>, [Accessed 13-08-2023].
- [38] I. Campbell Scientific, “The link budget and fade margin,” <https://s.campbellsci.com/documents/us/technical-papers/link-budget.pdf>, [Accessed 03-09-2023].
- [39] “Types of orbits — esa.int,” [https://www.esa.int/Enabling\\_Support/Space\\_Transportation/Types\\_of\\_orbits#:~:text=Low%20Earth%20orbit%20\(LEO\),-A%20low%20Earth&text=It%20is%20normally%20at%20an,very%20far%20above%20Earth's%20surface.](https://www.esa.int/Enabling_Support/Space_Transportation/Types_of_orbits#:~:text=Low%20Earth%20orbit%20(LEO),-A%20low%20Earth&text=It%20is%20normally%20at%20an,very%20far%20above%20Earth's%20surface.), [Accessed 12-08-2023].
- [40] electronicsforu, “Transmission basics: Designing a dipole antenna,” <https://www.electronicsforu.com/technology-trends/learn-electronics/transmission-basics-designing-dipole-antenna>, 2016, [Accessed 16-08-2023].

- [41] “Helix antennas,” <https://www.microwaves101.com/encyclopedia/helix-antennas>, 2018, [Accessed 16-08-2023].
- [42] C. P. SOLUTIONS, “Pcb layers explained: Multilayer boards and stackup rules,” <https://resourcespcb.cadence.com/blog/2019-pcb-layers-explained-multilayer-boards-and-stackup-rules>, [Accessed 18-08-2023].
- [43] Proteus, “Pcb via stitching and shielding,” <https://www.labcenter.com/blog/pcb-stitching-and-shielding/>, [Accessed 18-08-2023].
- [44] SFUPTOWNMAKER, “Pcb basics,” <https://learn.sparkfun.com/tutorials/pcb-basics/all>, [Accessed 18-08-2023].
- [45] A. Devices, “Pcb layout guidelines for rf and mixed signal,” <https://www.analog.com/en/technical-articles/pcbs-layout-guidelines-for-rf--mixedsignal.html>, [Accessed 18-08-2023].
- [46] N. T., “Standard 4- and 6-layer pcb stackups,” <https://www.bitweenie.com/listings/standard-4-and-6-layer-pcb-stackups/>, [Accessed 18-08-2023].
- [47] P. Electronics, “Routing guidelines for rf pcbs,” <https://www.proto-electronics.com/blog/routing-guidelines-rf-pcb>, [Accessed 29-09-2023].
- [48] J. D. Kraus, “Antennas for all applications,” [Accessed 29-09-2023].

# A. Project Planning

**Still to be formulated into a gantt chart** Week 01 (24/07 to 30/07): Problem formulation; requirements gathering Week 02 (31/07 to 06/08): Initial research; component selection Week 03 (07/08 to 13/08): System-level design; initial system layout; components ordered Week 04 (14/08 to 20/08): PCB design without traces; initial circuit design Week 05 (21/08 to 27/08): Component prototyping; Full PCB design; initial antenna design; Week 06 (28/08 to 03/09): Mechanical design; Custom link investigation; PCB ordered Week 07 (04/09 to 10/09): (Test week) Week 08 (11/09 to 17/09): Initial build Week 09 (18/09 to 24/09): Software design; initial testing Week 10 (25/09 to 01/10): Software design; debugging Week 11 (02/10 to 08/10): Reporting Week 12 (09/10 to 15/10): Design improvement Week 13 (16/10 to 22/10): Testing Week 14 (23/10 to 29/10): Reporting Week 15 (30/10 to 05/11):

# B. References

## B.1 PQSU

### Pocketcube Mechanical Interface

Dirk Slabber, MEng | Electronic Systems Laboratory | Stellenbosch University

13/06/2023

\* unless otherwise specified all measurements are to “The PocketQube Standard” [Issue 1, 7th of June, 2018], PQ9 and CS14 standard.

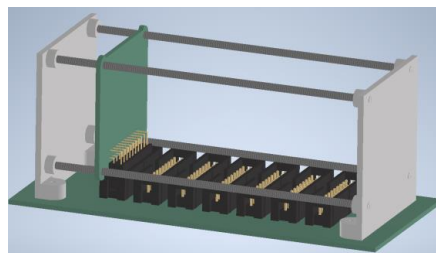


Figure 1- pocketcube structure

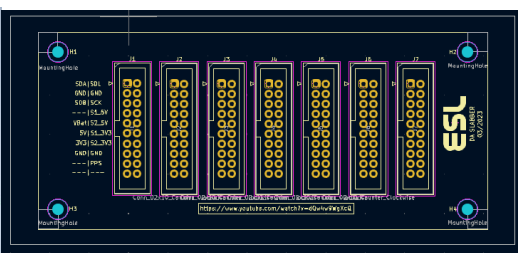


Figure 2- pocketcube bus layout

#### Physical Envelope

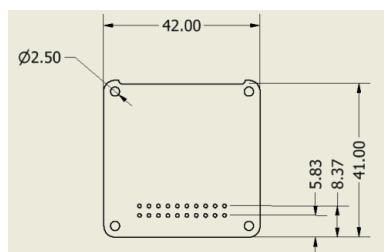


Figure 3-dimensions of the slot

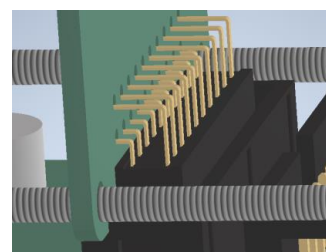


Figure 4-90-degree pins

Please take care to not place components such that it will obstruct the 90-degree bus pins as well as the nuts that will hold the slot in place around the four mounting holes. Components may project up to 8mm away from the board and still slot in with another board directly next to it.

#### Electrical Connection

Each slot is has twenty pins connected a bus in the main plate. Pin 1 is located top right on figure 3, pin 11 bottom right and so on. The suggested pinout on the bus is as follows:

1	SDA	SDL	11
2	Ground	Ground	12
3	SDB	System Clock	13
4	User defined	5V Switch 1	14
5	Power source	5V Switch 2	15
6	5V line	3.3V Switch 1	16
7	3.3 line	3.3V Switch 2	17
8	Ground	Ground	18
9	User defined	PPS	19
10	User defined	User defined	20

## B.2 SUNCQ

### SUNCQ Protocol

#### Commands

The following lists all commands from TNC to host and vice-versa. The command reservations are:

- 0x00 to 0x2F Host-to-TNC DO commands
- 0x30 to 0x5F Host-to-TNC SET commands
- 0x60 to 0x7F Host-to-TNC GET commands
- 0x80 to 0x9F TNC-to-Host STATUS replies
- 0xA0 to 0xCF TNC-to-Host DATA replies
- 0xD0 to 0xFE Reserved
- 0xFF Invalid

Code	Name	Function	Payload	Bytes	Comments
0x00	RESET	Reset the system	-	0	
0x01	CALIBRATE	Calibrate the system	-	0	Full calibration e.g. ground station and all sub-systems
0x02	RETURN_TO_START	Return the system to its starting state.	-	0	The starting state is post-calibration.
0x03	RETURN_TO_STOW	Return the system to its stow state.			The stow state is pre-calibration. Typically used before system shutdown
0x30	SET_TNC_MODE	Enter a TNC mode	See <i>TNC_MODE</i>	1	
0x31	SET_TRACK_MODE	Set tracking mode	See <i>TRACK_MODE</i>	1	
0x32	SET_PATH_DATA	Upload flight path data	CSV file. See <i>Flight Path Data</i> .	Any	The payload length is provided as the first 8 bytes.
0x33	SET_POINT_DIRECTION	Set the direction that the mount should point at			Only applicable when no tracking mode is selected
0x60	GET_SIGNAL_RSSI	Get RSSI of the signal	-	0	
0x61	GET_LOCATION	Get location of the ground station	Lat;Lng;Alt (f32:f32:f32)	12	
0x80	TNC_STATUS	Sent by the TNC as an ACK or status alert.	See <i>STATUS_CODE</i> .	1	Status 0x00 is used as an "ACK" command.
0x81	TNC_MESSAGE	Sent by the TNC to communicate a String message to the host.	char[]	Any	A newline character terminates the message
0xA0	SIGNAL_RSSI	Response to <i>GET_SIGNAL_RSSI</i>	float	4	
0xD0-0xFE	RESERVED	Reserved			Reserved for future use
0xFF	INVALID	Invalid			For internal use

## Details

### TNC\_MODE

Value	Description
0x00	Normal mode
0x01	KISS mode. This mode is exited using the KISS 0xFF command.

### TRACK\_MODE

The tracking mode is a combination flag i.e. multiple bits can be ORed together to specify that the payload must be tracked using multiple methods at once.

Value	Description
0x00	No tracking. Mount can be moved by setting the pointing vector.
0x01	Use uploaded GPS data
0x02	Use received GPS data (from payload)
0x04	Use signal strength, but only for an initial scan
0x08	Use signal strength, with dynamic conical scanning

### STATUS\_CODE

The following is a list of status codes that might be sent from the TNC to the host:

Value	Description
0x00	Acknowledge
0x01	Payload tracking unsuccessful/payload lost

### Flight path data

Flight path data can be uploaded in the form of a little-endian binary stream (i.e. each field should be least significant byte first). The first field is a 2-byte number indicating the number of flight path instances to follow. Then, the fields below should be provided. Such a file can be generated by predicting a flight path at <https://predict.sondehub.org/>, generating a CSV file, and then using the data to generate a binary stream. In the current implementation, only 200 entries are catered for – if longer flights are needed, then multiple streams should be set from the host intermittently. Time should be in Unix time (seconds since Epoch).

Name	Type
Time	uint64
Latitude	float32
Longitude	float32
Altitude	float32

## B.3 Antenna Gain

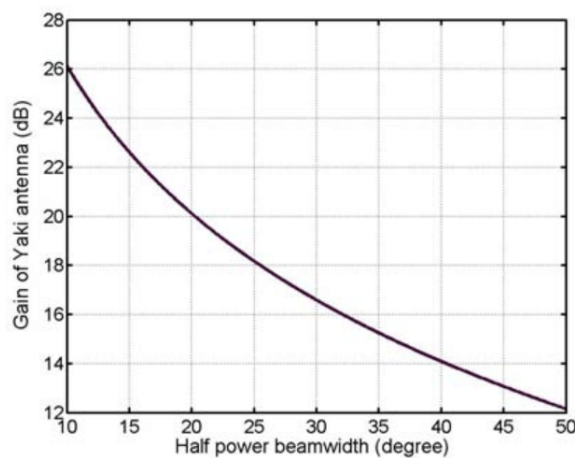
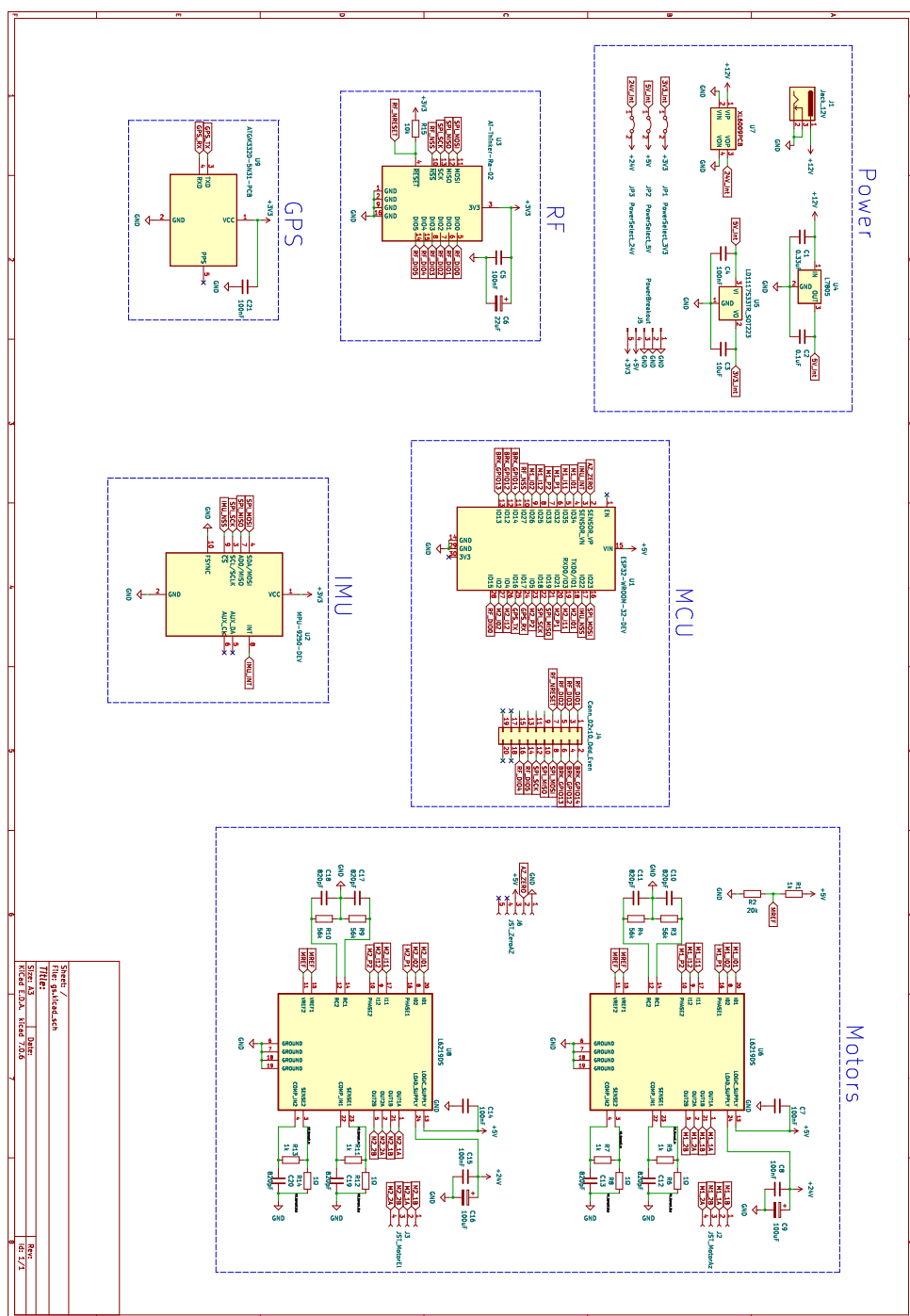


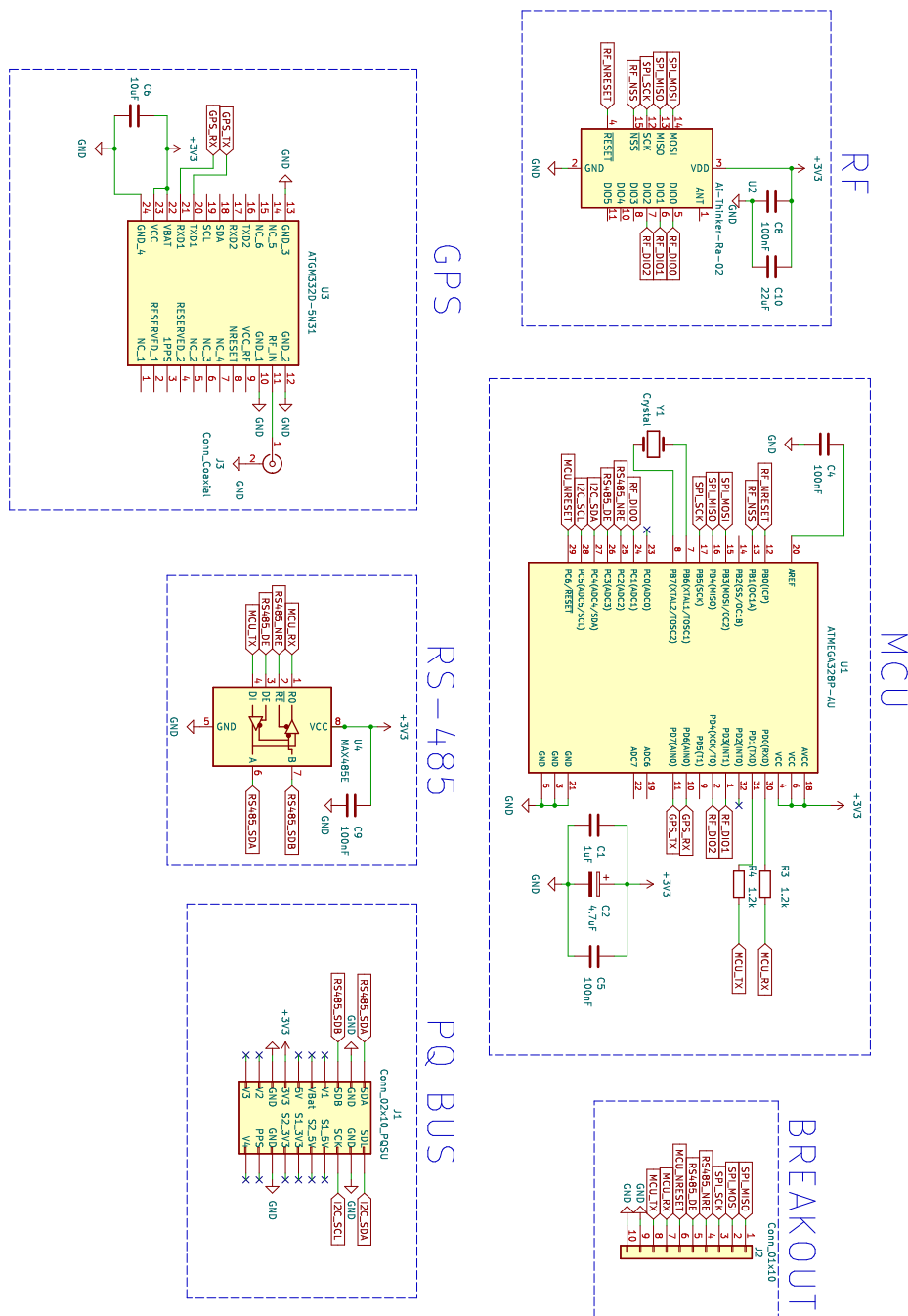
**Figure B.1:** Antenna Gain vs Beamwidth [7]

# C. Design

## C.1 Ground Station Schematic



## C.2 PocketQube Unit Schematic



### C.3 Ground Station PCB

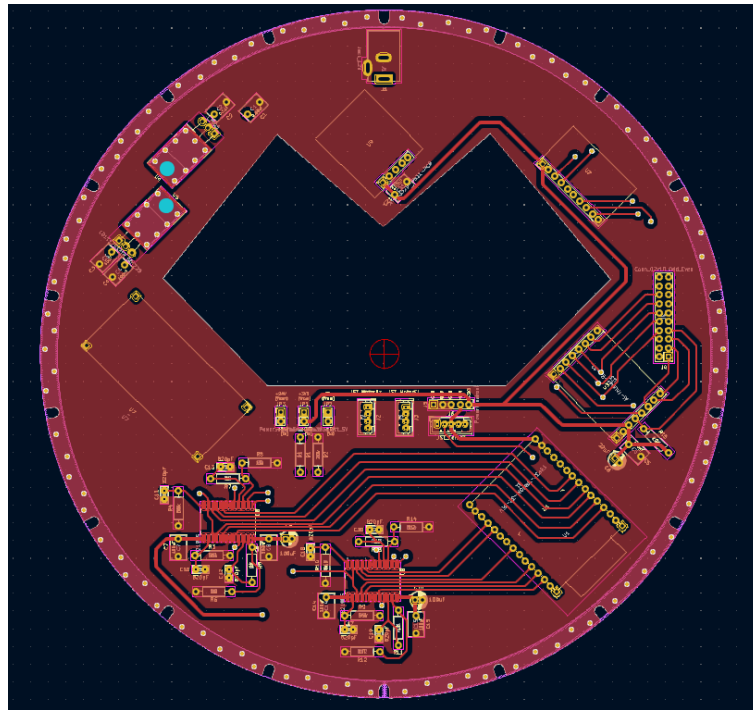


**Figure C.1:** Ground Station PCB Design

### C.4 PCB Errata

- Full errata for PCB designs still to be added

### C.5 Software

**Table C.1:** GPS Class

Function	Description
getLocation()	Return latitude, longitude and altitude
getTime()	Return seconds since epoch

**Table C.2:** Radio Class

Function	Description
startTransmit(message)	Transmit data (non-blocking i.e. with callback)
startReceive()	Start listening to receive data (non-blocking i.e. with callback)
getRssi()	Get signal strength
getSnr()	Get signal-to-noise ratio

**Table C.3:** Link Class

Function	Description
setTelemetryCallback(fn)	Set the "telemetry sent/received" function
setTelecommandCallback(fn)	Set the "telecommand received" function ( <i>Responder</i> only)

**Table C.4:** StepperMotor Class

Function	Description
stepForward(numSteps)	Blocking and non-blocking options
saveZeroPosition()	Used for calibration
getPosition()	Used for open-loop feedback
setSpeed()	Sets the delay between steps
setCurrentMultiplier()	Set the amount of current

**Table C.5:** Mount Class

Function	Description
calibrate()	Calibrate the mount
setAzimuthalElevation(az, el)	Set the azimuthal and elevation angles
setBoresight(boresightVec)	Set the boresight pointing vector

**Table C.6:** GroundStation Class

Function	Description
calibrate()	Calibrate the entire GS
addEstimatedLocation(loc)	Add an estimated input GPS location for open-loop tracking
addKnownLocation(loc)	Add a known GPS location for closed-loop tracking

# D. Hardware

## D.1 Existing Mount PCB



**Figure D.1:** Existing Antenna Mount PCB

## D.2 PocketQube

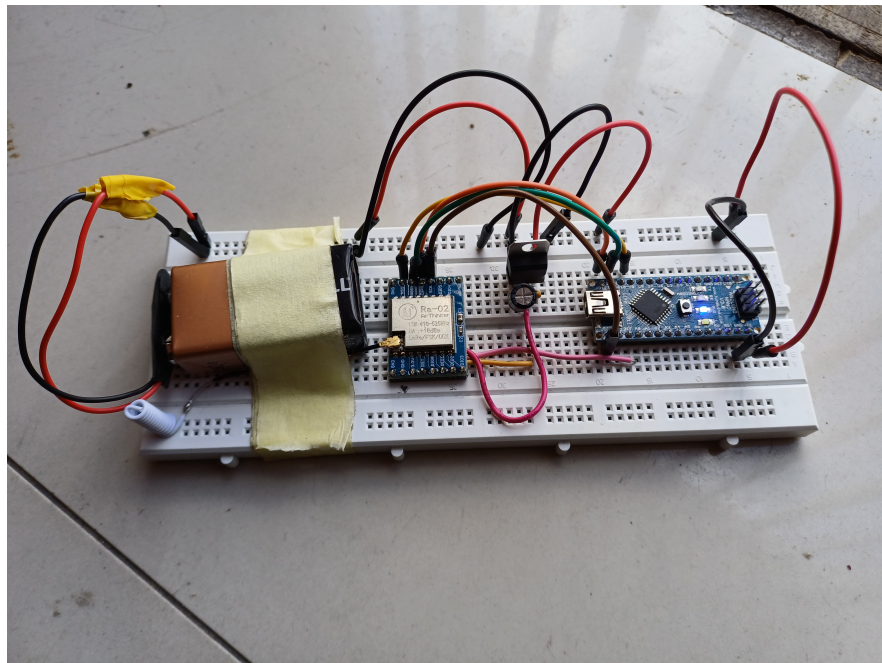


**Figure D.2:** PocketQube Breadboard for Testing



**Figure D.3:** PocketQube Dipole Antenna

### D.3 Mount Rotation



**Figure D.4:** Mount Azimuthal Compensation 1  
(Elevation Fixed)



**Figure D.5:** Mount Azimuthal Compensation 2  
(Elevation Fixed)



**Figure D.6:** Mount Azimuthal Compensation 3  
(Elevation Fixed)

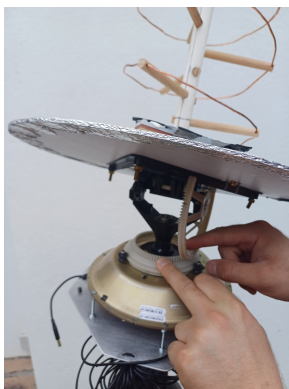


**Figure D.7:** Mount Azimuthal Compensation 4  
(Elevation Fixed)



**Figure D.8:** Mount Azimuthal Compensation 5  
(Azimuth Fixed)



**Figure D.9:** Mount Azimuthal Compensation 6  
(Azimuth Fixed)

# E. Software

## E.1 GUI

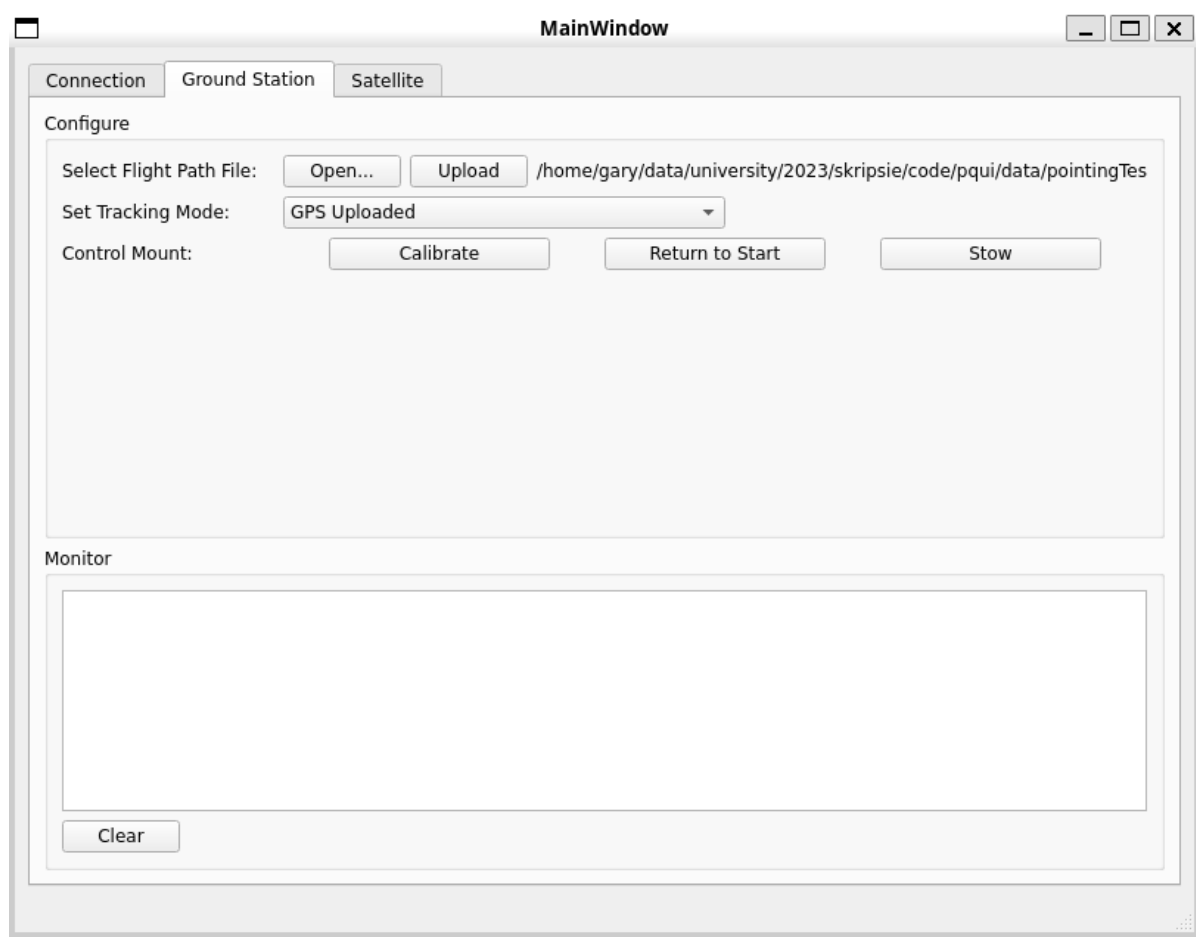


**Figure E.1:** GUI Snapshot

# F. Tests

## F.1 Range Tests

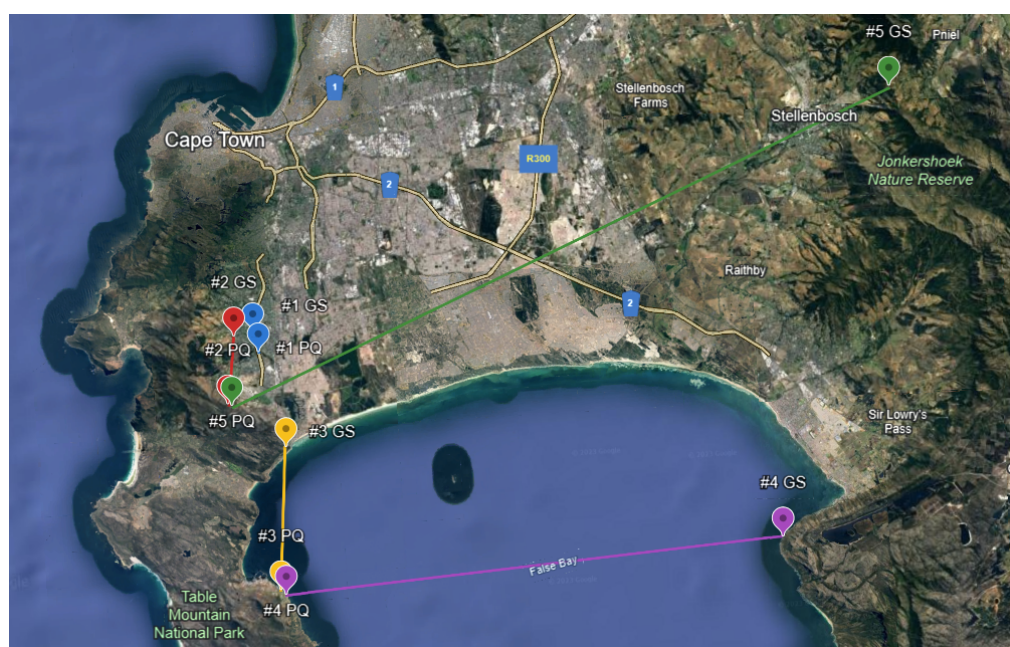


**Figure F.1:** Range Test Locations